Supporting Information for A DNA Small Molecular Probe with Increasing K^+ Concentration Promoted Selectivity

Ya-Ping Gong[a,b], Jian Yang,[c] Ji-Wang Fang[a,c], Qian Li[b], Zhi-Yong Yu[a*], Aijiao Guan[b*] and Han-Yuan Gong[c*]

[a]*Department of Chemistry, Renmin University of China, Beijing, 100872, P. R. China;* [b]*Institute of Chemistry, Chinese Academy of Sciences, Zhongguancunbeiyijie 2, Beijing 100190, P. R. China;* [c]*College of Chemistry, Beijing Normal University, Xinjiekouwaidajie 19, Beijing 100875, P. R. China.*

Zhi-Yong Yu: yuzhiyong@ruc.edu.cn;

Han-Yuan Gong: hanyuangong@bnu.edu.cn;

Aijiao Guan: ajguan@iccas.ac.cn

Content

Section S1: General considerations

All oligonucleotides (Table S1) were synthesized by Invitrogen (Beijing, China) and purified by ultra-polyacrylamide gel electrophoresis (ULTRAPAGE) (purity 95%). Spectral grade ethanol was purchased from Beijing Chem. Co. (China) and used without further purification. Ultrapure water prepared by Milli-Q Gradient ultrapure water system (Millipore) was used throughout the experiments.

Uv-vis absorbance experiment The absorption spectra were recorded on an Agilent 8453 UV-visible spectrophotometer at the wavelength range 190-1100 nm using a 1 cm quartz cuvette. Uv-vis absorbance titration were carried out by preparing a series of mixture containing **IPQC** and DNAs (The concentration of **IPQC** kept as 2.00×10^{-5} M, changing DNAs from 0 to 4.0 molar equiv., 0, 20 or 150 mM KCl added in the mixture containing ethanol and Tris-HCl buffer ([Tris] = 20 mM; the ratio between ethanol and aqueous phase as 1:99, *v/v*, pH = 7.2) at room temperature. Each absorption spectrum was carried out after the sample incubation for 2 h.

Fluorescence experiment Fluorescence spectra were recorded on a HITACHI F-4600 fluorescence spectrophotometer (Hitachi Limited, Japan). Fluorescence spectroscopic Job-plot was used to determine the binding stoichiometry. The total concentration of **IPQC** and DNAs were maintained as 2.00×10^{-5} M, with the molar ratio between **IPQC** and DNAs as 1:0, 5:1, 4:1, 3:1, 2:1, 1.5:1, 1:1, 1:1.5, 1:2, 1:3, 1:4 and 1:5, respectively. Fluorescence titration experiments were carried out with the same samples for the Uv-vis titration study.

CD (circular dichroism) experiment

CD spectra were collected on a Jasco 815 spectropolarimeter in a 2 mm path-length quartz cell. CD spectra of DNAs (2.00×10^{-5} M) were measured in the absence or presence of 1.0 molar equiv. of **IPQC**.

NMR experiment

^{1}H and ^{13}C NMR spectra were recorded on Bruker AVANCE 400.

X-ray experiment. The single crystals used to obtain the X-ray diffraction structure grew clear light red cube. The .cif documents are available as separate supporting

information files, which provide details regarding the specific crystal used for the analysis, along with the structure in question. Diffraction grade crystals were obtained via slow evaporation from solution using a mixture of dichloromethane / n-hexane.

The data samples were cut from the cluster of crystals and had the approximate dimensions given in the .cif document. The data were collected on Saturn724+ (2x2 bin mode) CCD diffractometers using agraphite monochromator with MoKa radiation (λ = 0.71073 Å). Data reduction was performed using CrystalClear. The structures were refined by full-matrix least-squares on F^2 with anisotropic displacement parameters for the non-H atoms using SHELXL-2014.[1] R(F), Rw(F^2) and the goodness of fit, S, are given below and in the .cif documents.[2] All ellipsoid figures were generated using SHELXTL/PC.[3] Positional and thermal parameters, bond lengths and angles, torsion angles, figures and lists of observed and calculated structure factors are located in the .cif document available from the Cambridge Crystallographic Data Centre (CCDC) by quoting the CCDC reference number 1977107. The .cif document also contains details of crystal data, data collection and structure refinement.

Section S2: **Synthesis and characterization of IPQC**

2-pyridylacetonitrile (0.24 g, 2 mmol), sodium bis(trimethylsilyl)-amide (NaHMDS) (0.55 g, 3 mmol) and anhydrous DMF (5 mL) were added into an oven-dried 25 mL Schleck tube and then heated at 100 °C for 3 h. Cooling the mixture down to room temperature, the mixture was filtered. After removing solvent under reduced pressure, the residue was purified by column chromatography on silica gel (200-300 mesh, eluent as the mixture of acetone and petroleum ether (1/3, *v*/*v*) to afford the corresponding product, a red-brown solid (0.42 g, 85% yield). ^{1}H NMR (400 MHz, Methanol-d_4) δ 9.42 (dt, J_1 = 7.4 Hz, J_2 = 1.1 Hz, 1H), 8.65 (ddd, J_1 = 4.9 Hz, J_2 = 1.8 Hz, J_3 = 1.0 Hz; 1H), 7.96 (s, 1H), 7.90 (ddd, J_1 = 8.1 Hz, J_2 = 7.3 Hz, J_3 =1.8 Hz; 1H), 7.84 (dt, J_1 = 8.2 Hz, J_2 = 1.1 Hz; 1H), 7.82 - 7.79 (m, 2H), 7.35 (ddd, J_1 = 7.3 Hz, J_2 = 4.9 Hz, J_3 = 1.3 Hz; 1H), 7.26 (ddd, J_1 = 7.4 Hz, J_2 = 4.8 Hz, J_3 = 3.4 Hz; 1H). ^{13}C NMR (100 MHz, Methanol-d_4) δ 157.0, 156.0, 149.0, 147.4, 138.5, 136.7, 134.9, 131.2, 123.5, 123.2(2C), 118.9, 117.2, 116.1, 81.0. ESI HRMS (*m/z*): calcd. for $C_{15}H_{10}N_4^{+\cdot}$ 246.0905; Found: 246.0903.

A possible two step reaction mechanism to obtain the product **IPQC** was suggested (Figure S1): 2-pyridylacetonitrile **1** provide a carbanion via deprotonation with additional base. Then carbanion reacts with *N*, *N*-dimethylformamide to construct a intermediate **2**[4],[5], after a further intramolecular cyclization of intermediate **2** with another carbanion under alkaline conditions [6], the goal product **IPQC** is given.

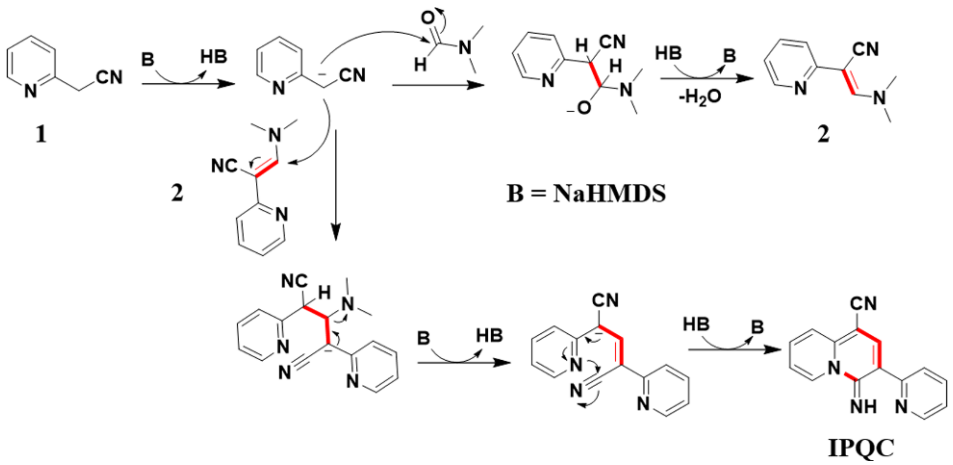

Figure S1 Proposed possible mechanism of **IPQC** synthesis.

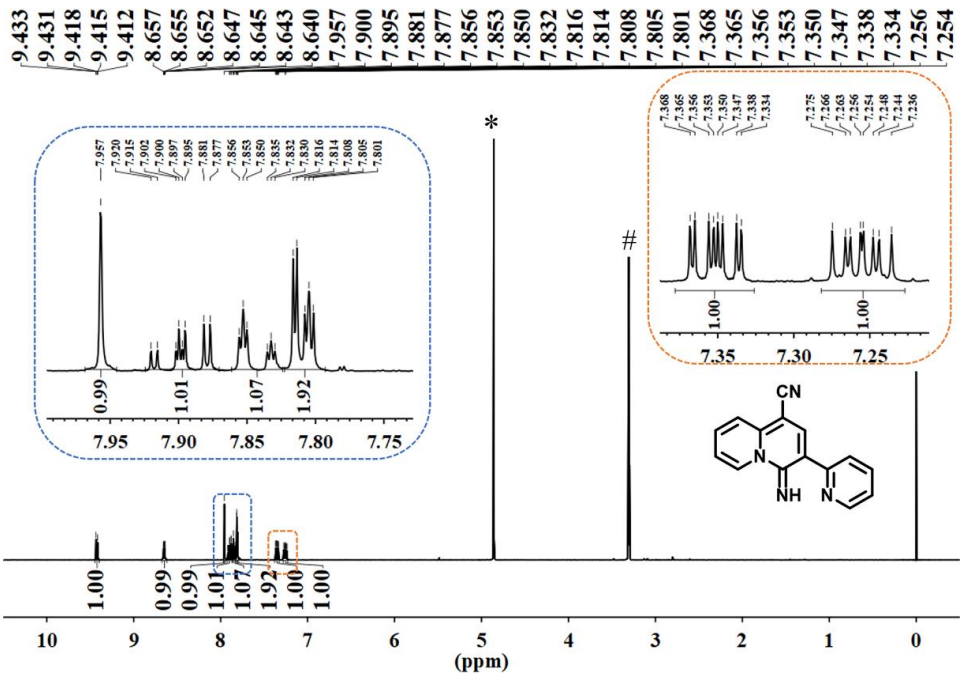

Figure S2 ^{1}H NMR spectrum of **IPQC** recorded in MeOH-d_4 (400 MHz, 298 K). ∗ is the residual signal of OH group on MeOH and H_2O. ♯ is the residual signal of Me group on MeOH.

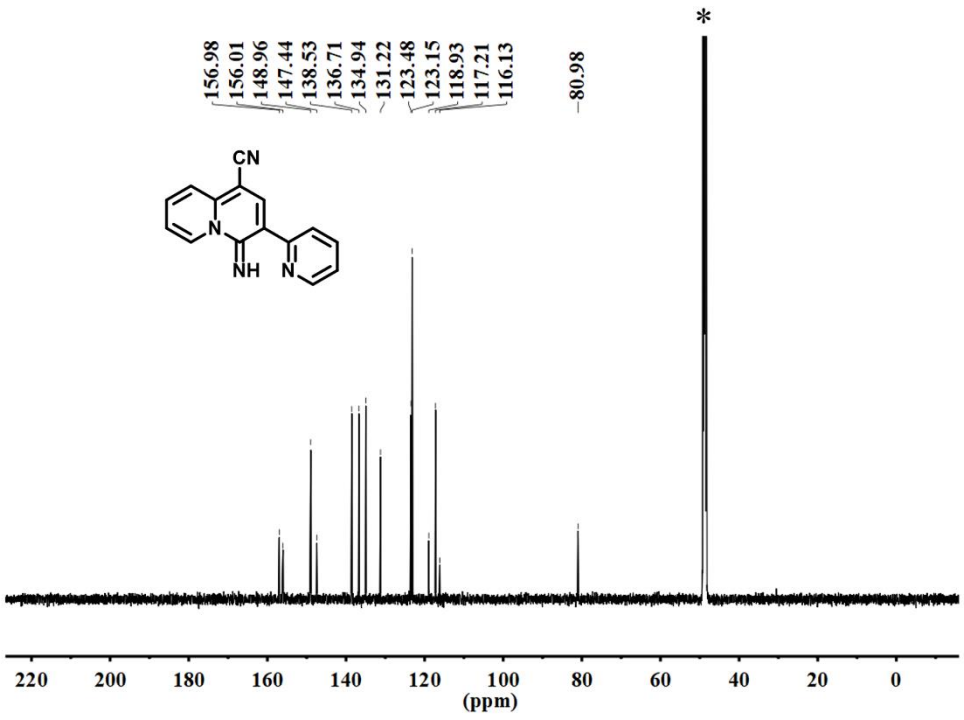

Figure S3 ^{13}C NMR spectrum of **IPQC** recorded in MeOH-d_4 (100 MHz, 298 K).

∗ is the signal of Me on MeOH.

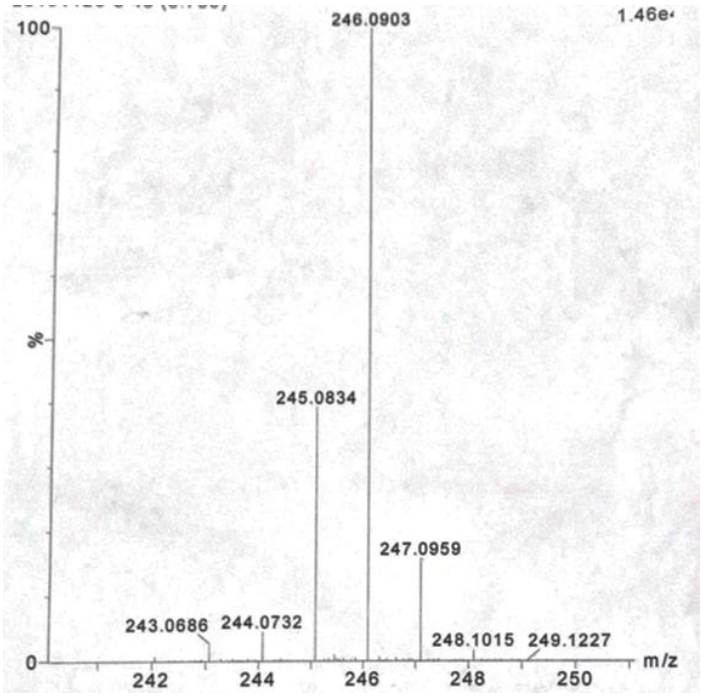

Figure S4 HRMS spectra of **IPQC**. calcd. for $C_{15}H_{10}N_4^{+\cdot}$ 246.0905; Found: 246.0903.

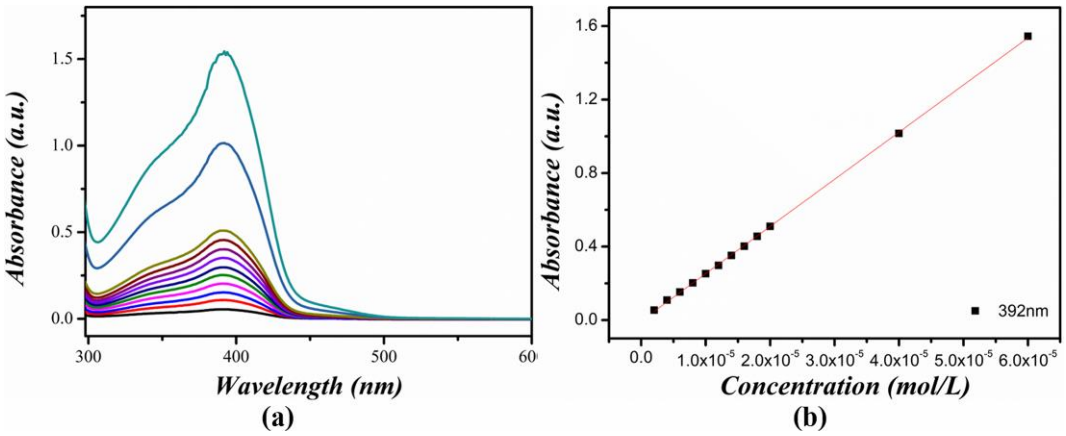

Figure S5 Concentration dependent Uv-vis absorption spectra (a) of **IPQC** and determination of molar absorption coefficient (from 2.00×10^{-6} to 6.00×10^{-5} M) in the mixture containing ethanol and Tris-HCl buffer ([Tris] = 20 mM; the ratio between ethanol and aqueous phase as 1:99, *v/v*, pH = 7.2). ε_{392nm} = 2.57×10^4 $mol^{-1} \cdot L \cdot cm^{-1}$ was given by linear fitting.

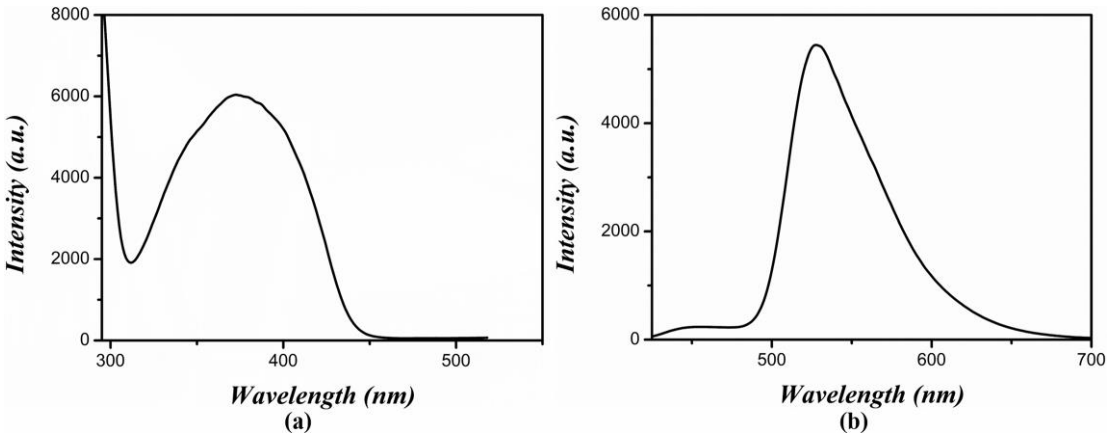

Figure S6 Fluorescence excitation (a, λ_{em} = 528 nm) and emission (b, λ_{ex} = 392 nm) spectra of 2.00 × 10^{-5} M **IPQC** in the mixture containing ethanol and Tris-HCl buffer ([Tris] = 20 mM; the ratio between ethanol and aqueous phase as 1:99, *v/v*, pH = 7.2) (voltage = 600 V, entrance slit width = 5 nm, exit slit width = 5 nm).

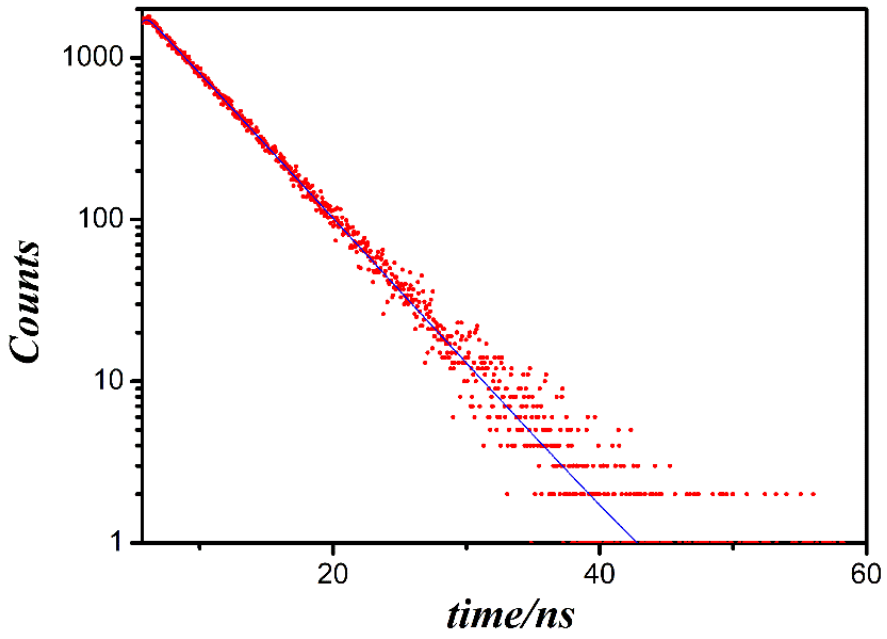

Figure S7 Fluorescence lifetime determination for **IPQC** (λ_{ex} = 392 nm, 2.00 × 10^{-5} M) in the mixture containing ethanol and Tris-HCl buffer ([Tris] = 20 mM; the ratio between ethanol and aqueous phase as 1:99, *v/v*, pH = 7.2). τ_f = 4.84 ns was caculated.

Section S3: **Single crystal X-ray structural analysis of IPQC.**

The crystallographic information and structural parameters of **IPQC** are as follows: clear light red, 0.08×0.03×0.03 mm^3; cube, space group P21/n; a = 6.8961(2), b = 12.3330(3), c = 13.6728(3) Å; α = 90, β = 96.385(2), γ = 90; V = 1155.65(5) $Å^3$; Z = 4; d = 1.415 g/cm^3; T = 100 K; R1 = 0.0369, wR2 = 0.1156 [I > 2ó(I)]; R1 = 0.0398, wR2 = 0.1201 (all data); S = 1.019; CCDC number: 1977107.

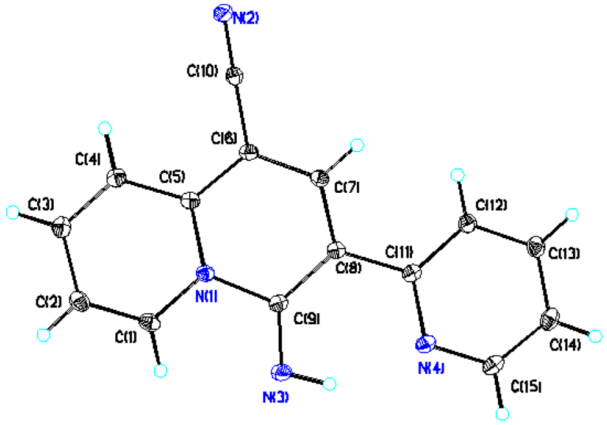

Figure S8 The single crystal structure of **IPQC**. Displacement are scaled to the 25% probability level.

Section S4: Sample preparation

The stock solutions of the oligonucleotides (sequences in Table S1) were prepared by dissolving oligonucleotides into the mixture containing ethanol and Tris-HCl buffer ([Tris] = 20 mM; the ratio between ethanol and aqueous phase as 1:99, *v/v*, pH = 7.2, containing 0, 20 or 150 mM KCl, respectively) and annealed in a thermocycler (first heating at 90 ^{o}C for 5 min, and cooled slowly to room temperature, then stored in 4 ^{o}C before use). The concentration of oligonucleotides was determined based on their absorbance at 260 nm, dsDNA was prepared by heat denaturing and annealing the mixture of ssDNA1 and ssDNA2 (1:1). Stock solutions of **IPQC** were prepared in ethanol (2.00×10^{-3} M).

Table S1 Oligonucleotide sequences used in the experiments

Name	Sequence (form 5'-3')	Type
ssPS1c-a	TTTTTTTTTTATTAAAATTTATAA	Single strand
ssPS1c-b	AAAAAAAAAATAATTTTAAATATT	Single strand
ssAf17	CTGAGTTGTATATATTCG	Single strand
ssG-tripl	GGTTGGTGTGG	Single strand
ssT30	TTTTTTTTTTTTTTTTTTTTTTTTTTTTT	Single strand
ssVEGF	GGGCGGGCCGGGGGCGGG	Single strand (no K^+)
dsPS1c	TTTTTTTTTTATTAAAATTTATAA	Double strand
	AAAAAAAAAATAATTTTAAATATT	
ds19AT	ACGTCGATTATAGACGAGC	Double strand
	GCTCGTCTATAATCGACGT	
dsDx12	GCGTGAGTTCGG	Double strand
	CCGAACTCACGC	
ds20	CGAATTCGTCTCCGAATTCG	Double strand
ds22	TTCGCGCGCGTTTTCGCGCGCG	Double strand
ds26	CAATCGGATCGAATTCGATCCGATTG	Double strand
hairpin15GC	GAAAAAAAAAAAAAGTTTTCTTTTTTTTTTTTC	Harpin
G4-bcl-2	GGGCGCGGGAGGAATTGGGCGGG	Hybrid G4(in K^+)
G4-H22	AGGGTTAGGGTTAGGGTTAGGG	Hybrid G4 (in K^+)
G4-VEGF	GGGCGGGCCGGGGGCGGG	Parallel G4 (in K^+)
G4-P21	GGGCCTGGGCCTGGGCCTGGG	Antiparallel G4 (in K^+)
G4-c-myc	AGGGTGGGGAGGGTGGGG	Parallel G4 (in K^+)
G4-c-kit	AGGGAGGGCGCTGGGAGGAGGG	Parallel G4 (in K^+)

Section S5: **The complexation study between IPQC and DNAs**

The complexation study between **IPQC** and G4 DNAs shown below was carried out in the mixture containing ethanol and Tris-HCl buffer ([KCl] = 20 mM, [Tris] = 20 mM; the ratio between ethanol and aqueous phase as 1:99, *v/v*, pH = 7.2).

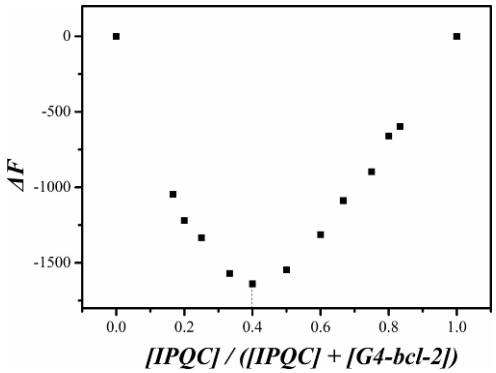

Figure S9 Job-plot corresponding to the interaction between **IPQC** and G4-bcl-2 at 298 K as monitored via fluorescence spectroscopy. In this study, [**IPQC**] + [G4-bcl-2] = 2.00 × 10^{-5} M, the minimum value of [**IPQC**] / ([**IPQC**] + [G4-bcl-2]) was found at 0.4, a finding consistent with a 2:3 (**IPQC**:G4-bcl-2) binding stoichiometry [7].

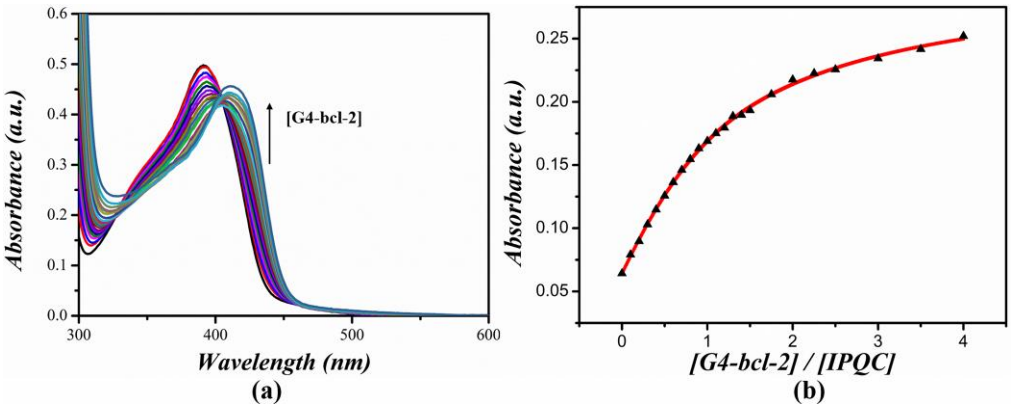

Figure S10 (a) Uv-vis absorption spectroscopic titration of **IPQC** (2.00 × 10^{-5} M) with G4-bcl-2 (0 to 4.0 molar equiv.); (b) change in the Uv-vis intensity data from 350 nm to 450 nm was used to calculate the K_{a1} = (5.0 ± 0.2) × 10^5 M^{-1}, K_{a2} = (7.9 ± 0.4) × 10^4 M^{-1}, K_{a3} = (3.2 ± 0.3) × 10^4 M^{-1} corresponding to the formation of **IPQC**·G4-bcl-2, **IPQC**·(G4-bcl-2)$_2$, (**IPQC**)$_2$·**(**G4-bcl-2)$_3$, using the Hyperquad 2003 program [8]. The red lines show the non-linear curve fit of the experimental data of 436 nm to the appropriate equation. Equations governing the relevant equilibria:

$$[H] + [G] \overset{K_{a1}}{\rightleftharpoons} [HG] \quad [HG] + [G] \overset{K_{a2}}{\rightleftharpoons} [HG_2] \quad [HG] + [HG_2] \overset{K_{a3}}{\rightleftharpoons} [H_2G_3]$$

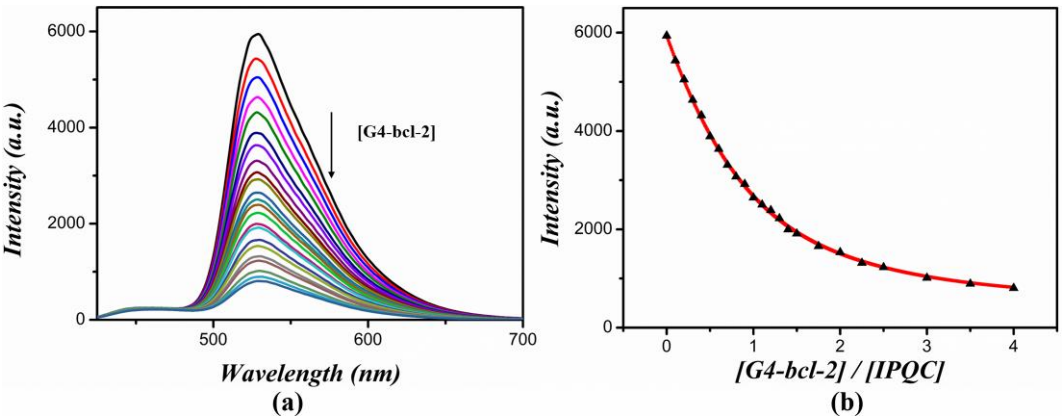

Figure S11 (a) Fluorescence spectroscopic titration of **IPQC** (2.00×10^{-5} M) with G4-bcl-2 (0 to 4.0 molar equiv.); (b) change in the intensity data from 425 nm to 700 nm was used to calculate the $K_{a1} = (2.5 \pm 0.1) \times 10^5$ M^{-1}, $K_{a2} = (1.3 \pm 0.1) \times 10^5$ M^{-1}, $K_{a3} = (2.0 \pm 0.2) \times 10^3$ M^{-1} corresponding to the formation of **IPQC**·G4-bcl-2, **IPQC**·$(G4\text{-bcl-2})_2$, $(\mathbf{IPQC})_2$·**(**$G4\text{-bcl-2})_3$, using the Hyperquad 2003 program [8]. The red lines show the non-linear curve fit of the experimental data of 528 nm to the appropriate equation. Equations governing the relevant equilibria: $[H] + [G] \overset{K_{a1}}{\rightleftharpoons} [HG]$

$[HG] + [G] \overset{K_{a2}}{\rightleftharpoons} [HG_2]$ $[HG] + [HG_2] \overset{K_{a3}}{\rightleftharpoons} [H_2G_3]$

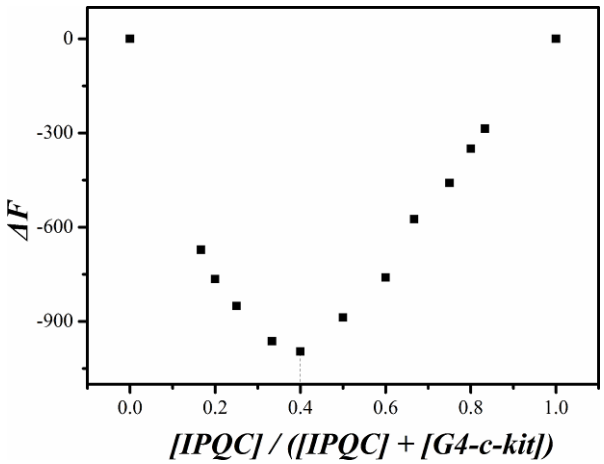

Figure S12 Job-plot corresponding to the interaction between **IPQC** and G4-c-kit at 298 K as monitored via fluorescence spectroscopy. In this study, [**IPQC**] + [G4-c-kit] = 2.00×10^{-5} M, the minimum value of [**IPQC**] / ([**IPQC**] + [G4-c-kit]) was found at 0.4, a finding consistent with a 2:3 (**IPQC**:G4-c-kit) binding stoichiometry [7].

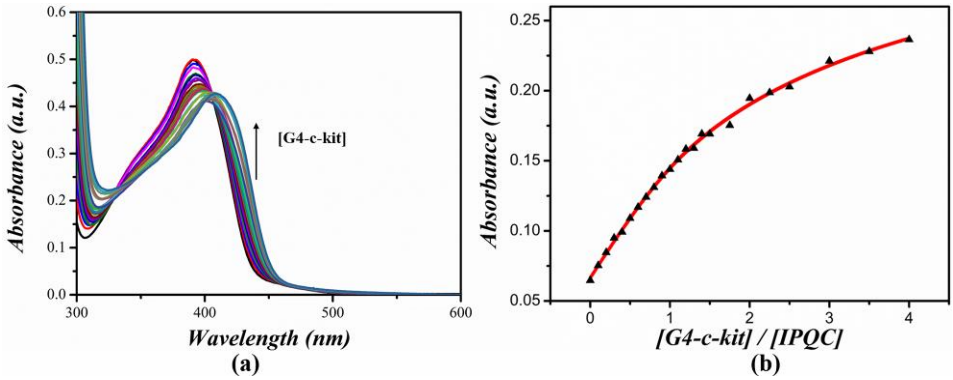

Figure S13 (a) Uv-vis absorption spectroscopic titration of **IPQC** (2.00×10^{-5} M) with G4-c-kit (0 to 4.0 molar equiv.); (b) change in the Uv-vis intensity data from 350 nm to 450 nm was used to calculate the $K_{a1} = (5.0 \pm 0.2) \times 10^5$ M^{-1}, $K_{a2} = (1.0 \pm 0.1) \times 10^4$ M^{-1}, $K_{a3} = (2.5 \pm 0.2) \times 10^3$ M^{-1} corresponding to the formation of **IPQC**·G4-c-kit, **IPQC**·(G4-c-kit)$_2$, (**IPQC**)$_2$·(G4-c-kit)$_3$, using the Hyperquad 2003 program [8]. The red lines show the non-linear curve fit of the experimental data of 436 nm to the appropriate equation. Equations governing the relevant equilibria: $[H] + [G] \overset{K_{a1}}{\rightleftharpoons} [HG]$ $[HG] + [G] \overset{K_{a2}}{\rightleftharpoons} [HG_2]$ $[HG] + [HG_2] \overset{K_{a3}}{\rightleftharpoons} [H_2G_3]$

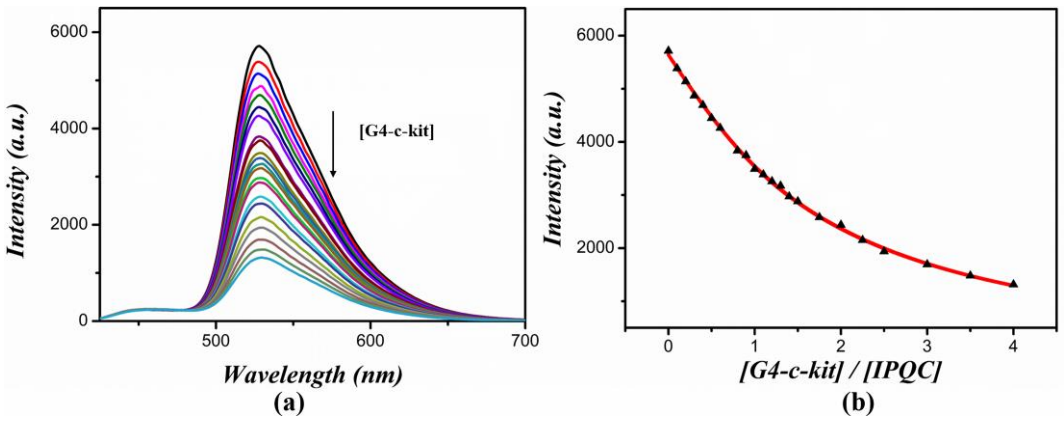

Figure S14 (a) Fluorescence spectroscopic titration of **IPQC** (2.00×10^{-5} M) with G4-c-kit (0 to 4.0 molar equiv.); (b) change in the intensity data from 425 nm to 700 nm was used to calculate the $K_{a1} = (3.2 \pm 0.1) \times 10^5$ M^{-1}, $K_{a2} = (7.9 \pm 0.4) \times 10^3$ M^{-1}, $K_{a3} = (5.0 \pm 0.4) \times 10^3$ M^{-1} corresponding to the formation of **IPQC**·G4-c-kit, **IPQC**·(G4-c-kit)$_2$, (**IPQC**)$_2$·(G4-c-kit)$_3$, using the Hyperquad 2003 program [8]. The red lines show the non-linear curve fit of the experimental data of 528 nm to the appropriate equation. Equations governing the relevant equilibria: $[H] + [G] \overset{K_{a1}}{\rightleftharpoons} [HG]$ $[HG] + [G] \overset{K_{a2}}{\rightleftharpoons} [HG_2]$ $[HG] + [HG_2] \overset{K_{a3}}{\rightleftharpoons} [H_2G_3]$

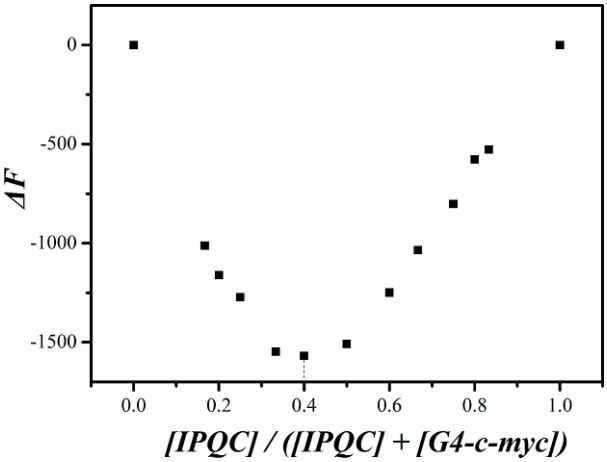

Figure S15 Job-plot corresponding to the interaction between **IPQC** and G4-c-myc at 298 K as monitored via fluorescence spectroscopy. In this study, [**IPQC**] + [G4-c-myc] = 2.00 × 10^{-5} M, the minimum value of [**IPQC**] / ([**IPQC**] + [G4-c-myc]) was found at 0.4, a finding consistent with a 2:3 (**IPQC**:G4-c-myc) binding stoichiometry [7].

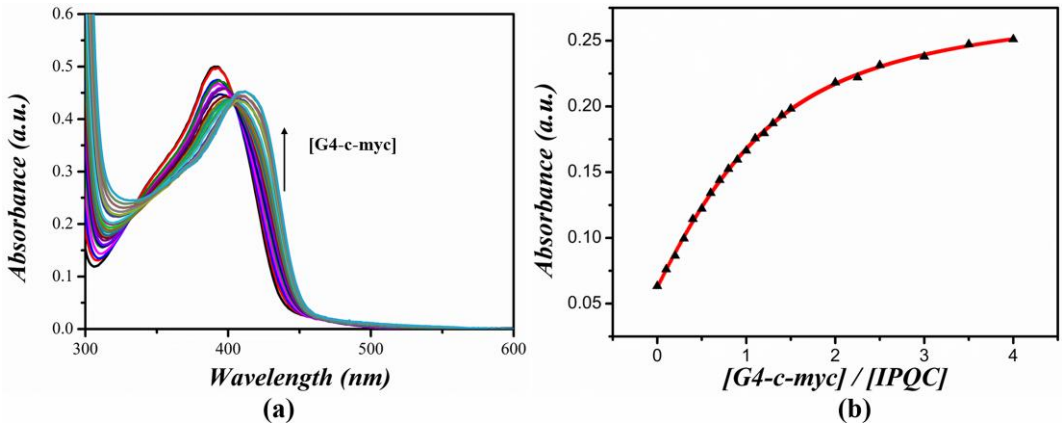

Figure S16 (a) Uv-vis absorption spectroscopic titration of **IPQC** (2.00 × 10^{-5} M) with G4-c-myc (0 to 4.0 molar equiv.); (b) change in the Uv-vis intensity data from 350 nm to 450 nm was used to calculate the K_{a1} = (6.3 ± 0.2) × 10^5 M^{-1}, K_{a2} = (1.0 ± 0.1) × 10^5 M^{-1}, K_{a3} = (5.0 ± 0.4) × 10^4 M^{-1} corresponding to the formation of **IPQC**·G4-c-myc, **IPQC**·(G4-c-myc)$_2$, (**IPQC**)$_2$·(G4-c-myc)$_3$, using the Hyperquad 2003 program [8]. The red lines show the non-linear curve fit of the experimental data of 436 nm to the appropriate equation. Equations governing the relevant equilibria:

$$[H] + [G] \overset{K_{a1}}{\rightleftharpoons} [HG] \qquad [HG] + [G] \overset{K_{a2}}{\rightleftharpoons} [HG_2] \qquad [HG] + [HG_2] \overset{K_{a3}}{\rightleftharpoons} [H_2G_3]$$

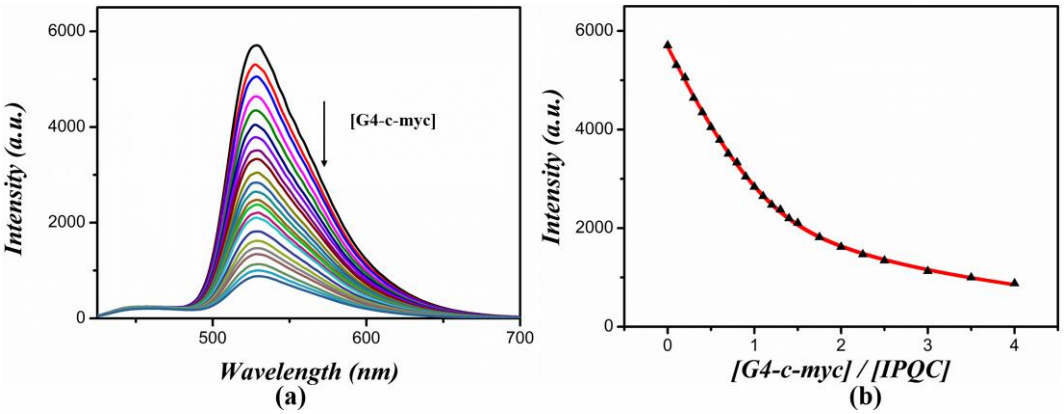

Figure S17 (a) Fluorescence spectroscopic titration of **IPQC** (2.00×10^{-5} M) with G4-c-myc (0 to 4.0 molar equiv.); (b) change in the intensity data from 425 nm to 700 nm was used to calculate the $K_{a1} = (7.9 \pm 0.2) \times 10^5$ M^{-1}, $K_{a2} = (3.2 \pm 0.2) \times 10^4$ M^{-1}, $K_{a3} = (2.0 \pm 0.2) \times 10^5$ M^{-1} corresponding to the formation of **IPQC**·G4-c-myc, **IPQC**·(G4-c-myc)$_2$, (**IPQC**)$_2$·(G4-c-myc)$_3$, using the Hyperquad 2003 program [8]. The red lines show the non-linear curve fit of the experimental data of 528 nm to the appropriate equation. Equations governing the relevant equilibria: $[H] + [G] \overset{K_{a1}}{\rightleftharpoons} [HG]$ $[HG] + [G] \overset{K_{a2}}{\rightleftharpoons} [HG_2]$ $[HG] + [HG_2] \overset{K_{a3}}{\rightleftharpoons} [H_2G_3]$

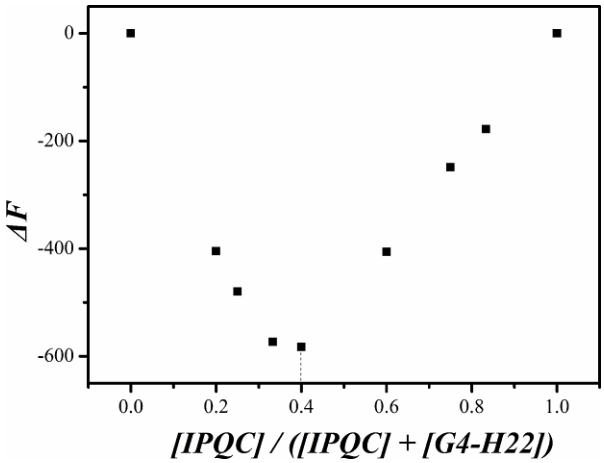

Figure S18 Job-plot corresponding to the interaction between **IPQC** and G4-H22 at 298 K as monitored via fluorescence spectroscopy. In this study, [**IPQC**] + [G4-H22] = 2.00×10^{-5} M, the minimum value of [**IPQC**] / ([**IPQC**] + [G4-H22]) was found at 0.4, a finding consistent with a 2:3 (**IPQC**:G4-H22) binding stoichiometry [7].

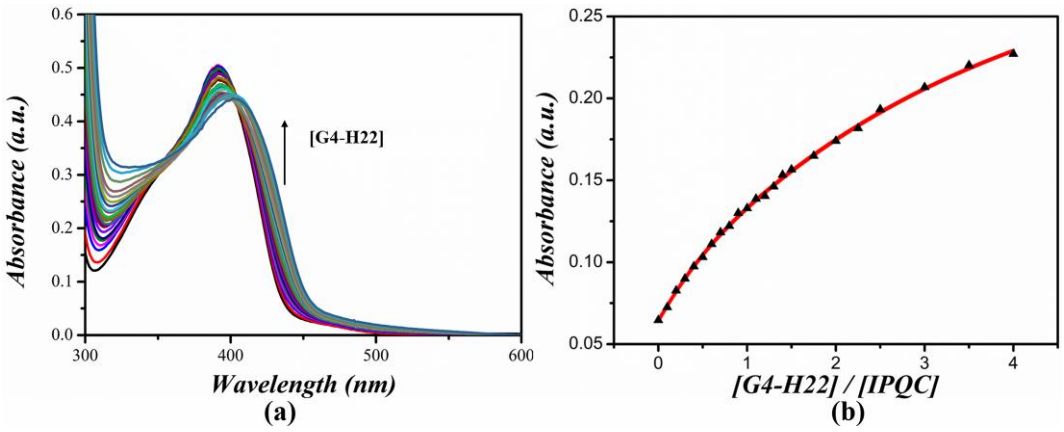

Figure S19 (a) Uv-vis absorption spectroscopic titration of **IPQC** (2.00×10^{-5} M) with G4-H22 (0 to 4.0 molar equiv.); (b) change in the Uv-vis intensity data from 350 nm to 450 nm was used to calculate the $K_{a1} = (7.9 \pm 0.2) \times 10^4$ M^{-1}, $K_{a2} = (6.3 \pm 0.3) \times 10^4$ M^{-1}, $K_{a3} = (2.0 \pm 0.2) \times 10^5$ M^{-1} corresponding to the formation of **IPQC**·G4-H22, **IPQC**·(G4-H22)$_2$, (**IPQC**)$_2$·(G4-H22)$_3$, using the Hyperquad 2003 program [8]. The red lines show the non-linear curve fit of the experimental data of 436 nm to the appropriate equation. Equations governing the relevant equilibria: $[H] + [G] \overset{K_{a1}}{\rightleftharpoons} [HG]$ $[HG] + [G] \overset{K_{a2}}{\rightleftharpoons} [HG_2]$ $[HG] + [HG_2] \overset{K_{a3}}{\rightleftharpoons} [H_2G_3]$

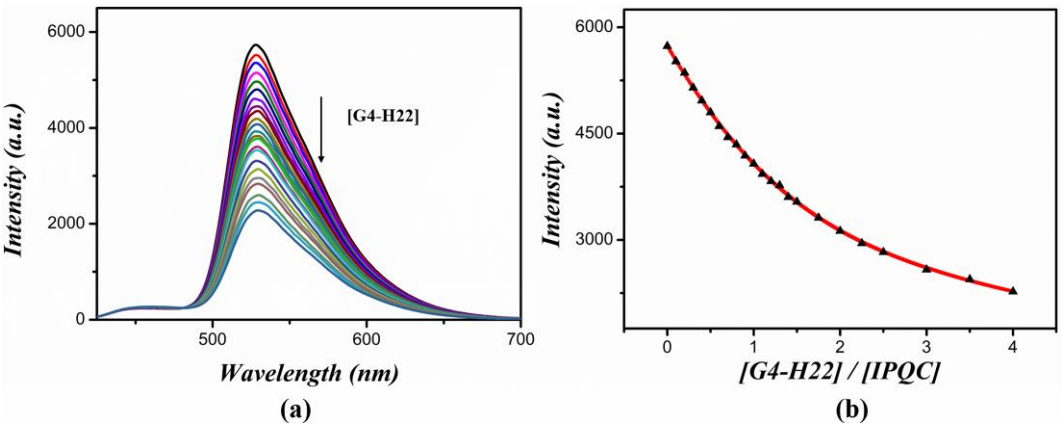

Figure S20 (a) Fluorescence spectroscopic titration of **IPQC** (2.00×10^{-5} M) with G4-H22 (0 to 4.0 molar equiv.); (b) change in the intensity data from 425 nm to 700 nm was used to calculate the $K_{a1} = (1.0 \pm 0.1) \times 10^5$ M^{-1}, $K_{a2} = (2.5 \pm 0.1) \times 10^4$ M^{-1}, $K_{a3} = (7.9 \pm 0.6) \times 10^4$ M^{-1} corresponding to the formation of **IPQC**·G4-H22, **IPQC**·(G4-H22)$_2$, (**IPQC**)$_2$·(G4-H22)$_3$, using the Hyperquad 2003 program [8]. The

red lines show the non-linear curve fit of the experimental data of 528 nm to the appropriate equation. Equations governing the relevant equilibria: $[H] + [G] \overset{K_{a1}}{\rightleftharpoons} [HG]$ $[HG] + [G] \overset{K_{a2}}{\rightleftharpoons} [HG_2]$ $[HG] + [HG_2] \overset{K_{a3}}{\rightleftharpoons} [H_2G_3]$

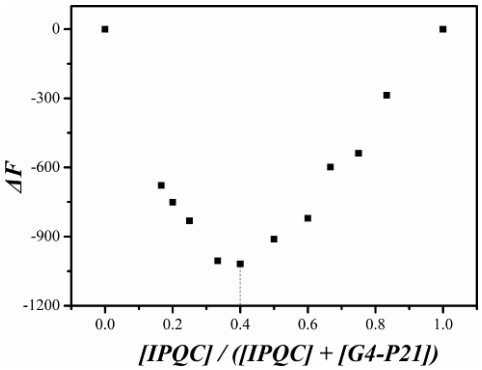

Figure S21 Job-plot corresponding to the interaction between **IPQC** and G4-P21 at 298 K as monitored via fluorescence spectroscopy. In this study, [**IPQC**] + [G4-P21] = 2.00×10^{-5} M, the minimum value of [**IPQC**] / ([**IPQC**] + [G4-P21]) was found at 0.4, a finding consistent with a 2:3 (**IPQC**:G4-P21) binding stoichiometry [7].

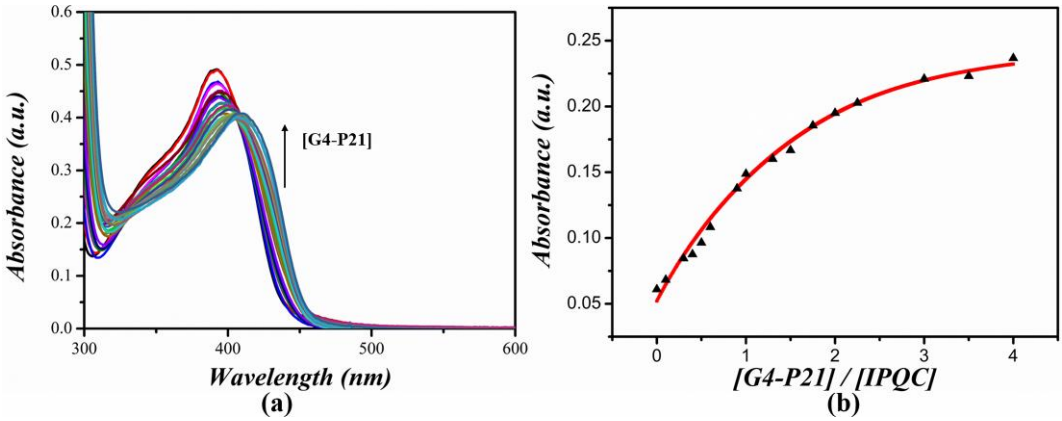

Figure S22 (a) Uv-vis absorption spectroscopic titration of **IPQC** (2.00×10^{-5} M) with G4-P21 (0 to 4.0 molar equiv.); (b) change in the Uv-vis intensity data from 350 nm to 450 nm was used to calculate the $K_{a1} = (7.9 \pm 0.2) \times 10^4$ M^{-1}, $K_{a2} = (1.3 \pm 0.1) \times 10^5$ M^{-1}, $K_{a3} = (2.5 \pm 0.2) \times 10^4$ M^{-1} corresponding to the formation of **IPQC**·G4-P21, **IPQC**·(G4-P21)$_2$, (**IPQC**)$_2$·(G4-P21)$_3$, using the Hyperquad 2003 program [8]. The red lines show the non-linear curve fit of the experimental data of 436 nm to the appropriate equation. Equations governing the relevant equilibria: $[H] + [G] \overset{K_{a1}}{\rightleftharpoons} [HG]$ $[HG] + [G] \overset{K_{a2}}{\rightleftharpoons} [HG_2]$ $[HG] + [HG_2] \overset{K_{a3}}{\rightleftharpoons} [H_2G_3]$

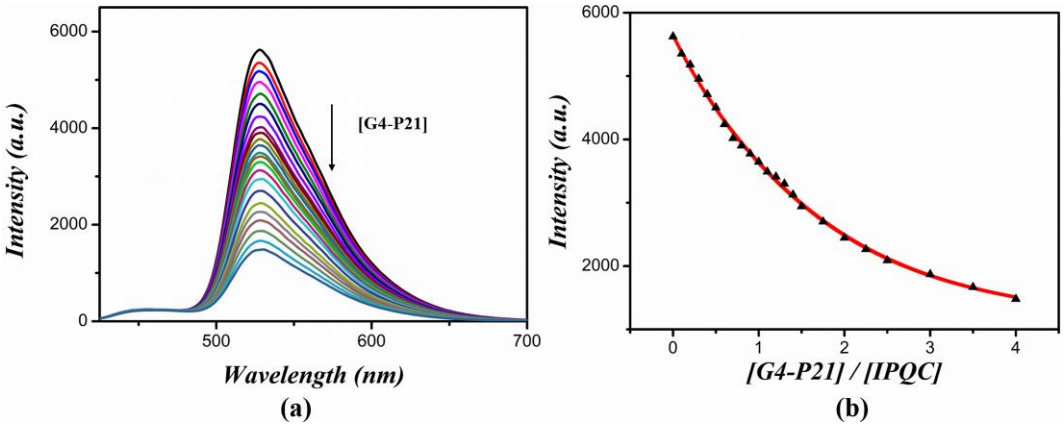

Figure S23 (a) Fluorescence spectroscopic titration of **IPQC** (2.00×10^{-5} M) with G4-P21 (0 to 4.0 molar equiv.); (b) change in the intensity data from 425 nm to 700 nm was used to calculate the $K_{a1} = (7.9 \pm 0.2) \times 10^4$ M^{-1}, $K_{a2} = (1.3 \pm 0.1) \times 10^5$ M^{-1}, $K_{a3} = (2.5 \pm 0.2) \times 10^4$ M^{-1} corresponding to the formation of **IPQC**·G4-P21, **IPQC**·(G4-P21)$_2$, (**IPQC**)$_2$·(G4-P21)$_3$, using the Hyperquad 2003 program [8]. The red lines show the non-linear curve fit of the experimental data of 528 nm to the appropriate equation. Equations governing the relevant equilibria: $[H] + [G] \overset{K_{a1}}{\rightleftharpoons} [HG]$ $[HG] + [G] \overset{K_{a2}}{\rightleftharpoons} [HG_2]$ $[HG] + [HG_2] \overset{K_{a3}}{\rightleftharpoons} [H_2G_3]$

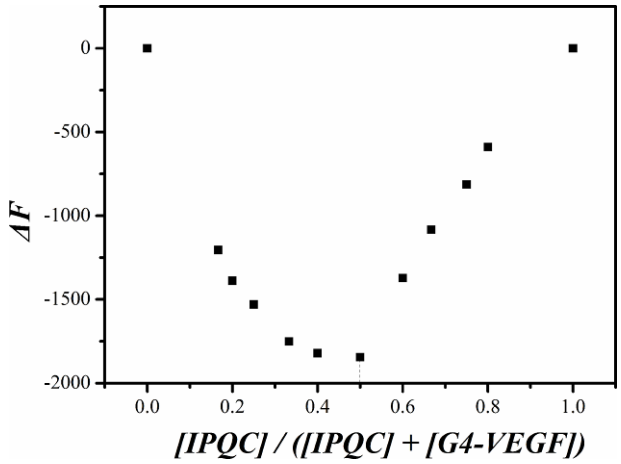

Figure S24 Job-plot corresponding to the interaction between **IPQC** and G4-VEGF at 298 K as monitored via fluorescence spectroscopy. In this study, [**IPQC**] + [G4-VEGF] = 2.00×10^{-5} M, the minimum value of [**IPQC**] / ([**IPQC**] + [G4-VEGF]) was found at 0.5, a finding consistent with a 1:1 (**IPQC**:G4-VEGF) binding stoichiometry [7].

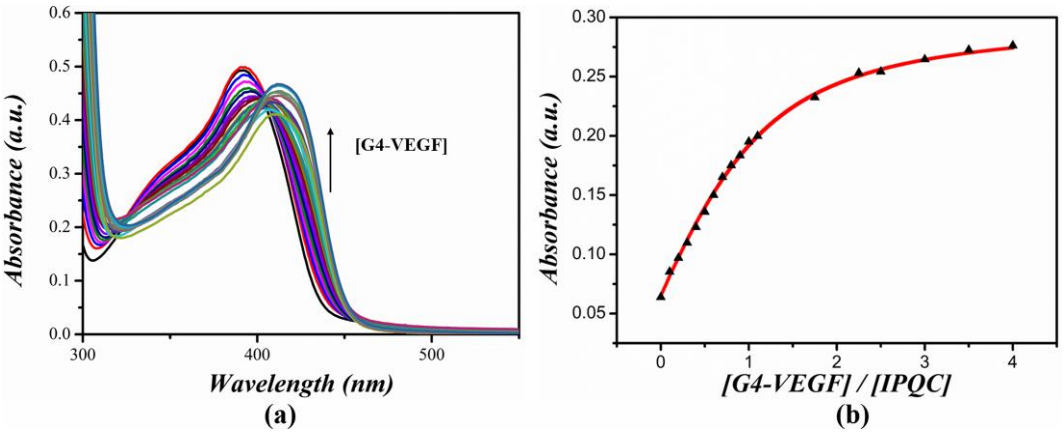

Figure S25 (a) Uv-vis absorption spectroscopic titration of **IPQC** (2.00×10^{-5} M) with G4-VEGF (0 to 4.0 molar equiv.); (b) change in the Uv-vis intensity data from 350 nm to 450 nm was used to calculate the K_{a1} = (1.3 ± 0.1) × 10^5 M^{-1}, corresponding to the formation of **IPQC**·G4-VEGF, using the Hyperquad 2003 program [8]. The red lines show the non-linear curve fit of the experimental data of 436 nm to the appropriate equation. Equations governing the relevant equilibria: $[H] + [G] \overset{K_{a1}}{\rightleftharpoons} [HG]$

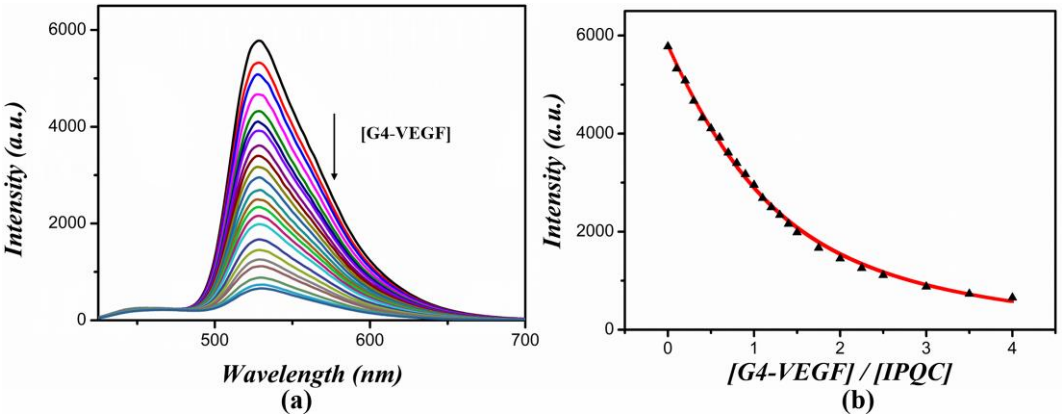

Figure S26 (a) Fluorescence spectroscopic titration of **IPQC** (2.00×10^{-5} M) with G4-VEGF (0 to 4.0 molar equiv.); (b) change in the intensity data from 425 nm to 700 nm was used to calculate the K_{a1} = (7.9 ± 0.2) × 10^4 M^{-1} corresponding to the formation of **IPQC**·G4-VEGF, using the Hyperquad 2003 program [8]. The red lines show the non-linear curve fit of the experimental data of 528 nm to the appropriate equation. Equations governing the relevant equilibria: $[H] + [G] \overset{K_{a1}}{\rightleftharpoons} [HG]$

The complexation study between **IPQC** and ss/ds DNAs shown below was carried out in the mixture containing ethanol and Tris-HCl buffer ([KCl] = 0 mM, [Tris] = 20 mM; the ratio between ethanol and aqueous phase as 1:99, *v/v*, pH = 7.2).

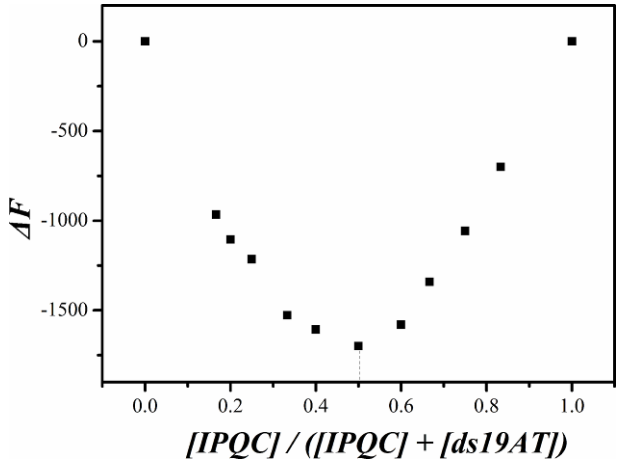

Figure S27 Job-plot corresponding to the interaction between **IPQC** and ds19AT at 298 K as monitored via fluorescence spectroscopy. In this study, [**IPQC**] + [ds19AT] = 2.00×10^{-5} M, the minimum value of [**IPQC**] / ([**IPQC**] + [ds19AT]) was found at 0.5, a finding consistent with a 1:1 (**IPQC**:ds19AT) binding stoichiometry [7].

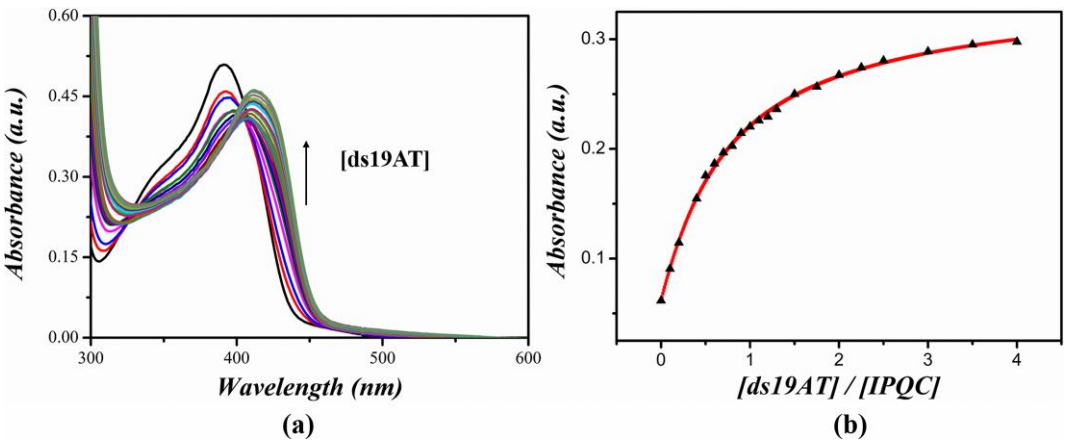

Figure S28 (a) Uv-vis absorption spectroscopic titration of **IPQC** (2.00×10^{-5} M) with ds19AT (0 to 4.0 molar equiv.); (b) change in the Uv-vis intensity data from 350 nm to 450 nm was used to calculate the $K_{a1} = (3.2 \pm 0.1) \times 10^4$ M^{-1} corresponding to the formation of **IPQC**·ds19AT, using the Hyperquad 2003 program [8]. The red lines show the non-linear curve fit of the experimental data of 436 nm to the appropriate equation. Equations governing the relevant equilibria: $[H] + [G] \overset{K_{a1}}{\rightleftharpoons} [HG]$

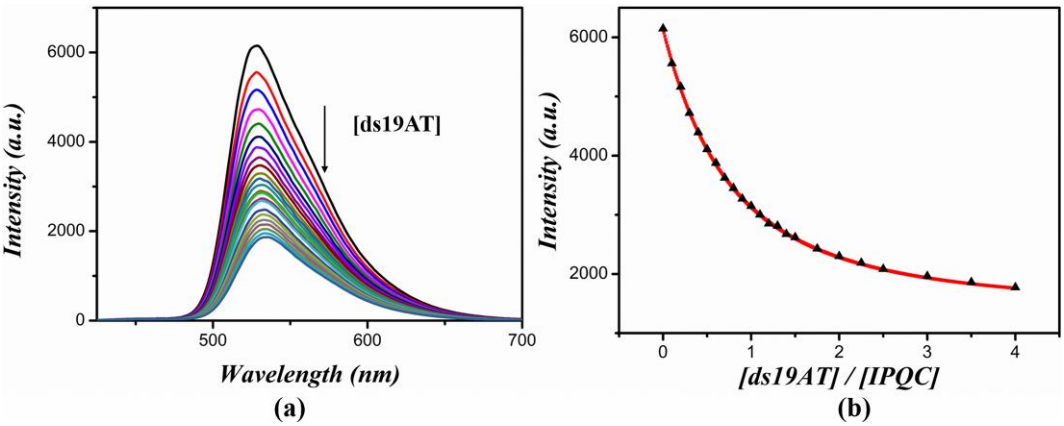

Figure S29 (a) Fluorescence spectroscopic titration of **IPQC** (2.00×10^{-5} M) with ds19AT (0 to 4.0 molar equiv.); (b) change in the intensity data from 425 nm to 700 nm was used to calculate the K_{a1} = (3.2 ± 0.1) × 10^4 M^{-1} corresponding to the formation of **IPQC**·ds19AT, using the Hyperquad 2003 program [8]. The red lines show the non-linear curve fit of the experimental data of 528 nm to the appropriate equation. Equations governing the relevant equilibria: $[H] + [G] \overset{K_{a1}}{\rightleftharpoons} [HG]$

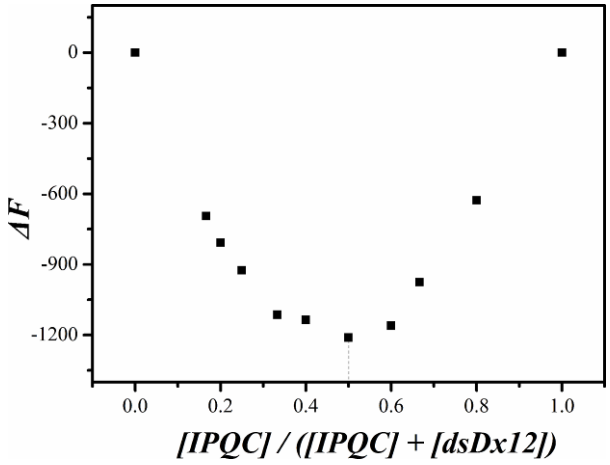

Figure S30 Job-plot corresponding to the interaction between **IPQC** and dsDx12 at 298 K as monitored via fluorescence spectroscopy. In this study, [**IPQC**] + [dsDx12] = 2.00×10^{-5} M, the minimum value of [**IPQC**] / ([**IPQC**] + [dsDx12]) was found at 0.5, a finding consistent with a 1:1 (**IPQC**:dsDx12) binding stoichiometry [7].

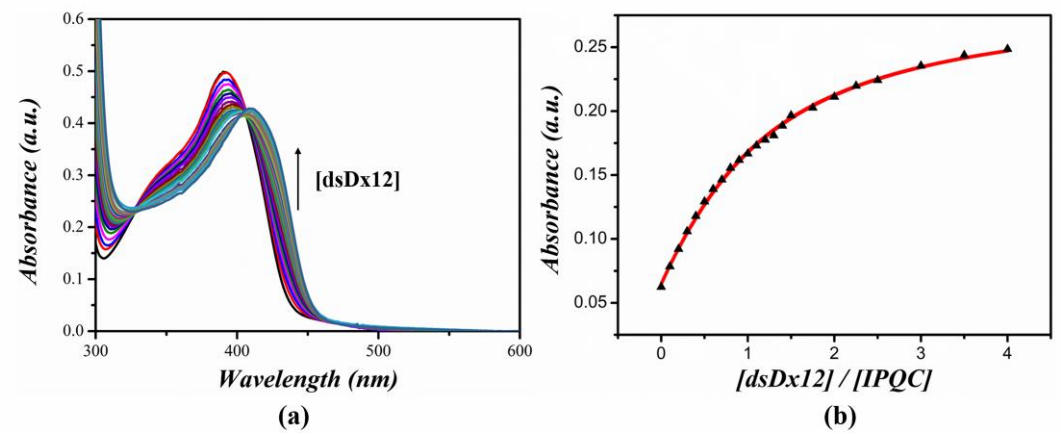

Figure S31 (a) Uv-vis absorption spectroscopic titration of **IPQC** (2.00×10^{-5} M) with dsDx12 (0 to 4.0 molar equiv.); (b) change in the Uv-vis intensity data from 350 nm to 450 nm was used to calculate the $K_{a1} = (7.9 \pm 0.2) \times 10^4$ M^{-1} corresponding to the formation of **IPQC**·dsDx12, using the Hyperquad 2003 program [8]. The red lines show the non-linear curve fit of the experimental data of 436 nm to the appropriate equation. Equations governing the relevant equilibria: $[H] + [G] \overset{K_{a1}}{\rightleftharpoons} [HG]$

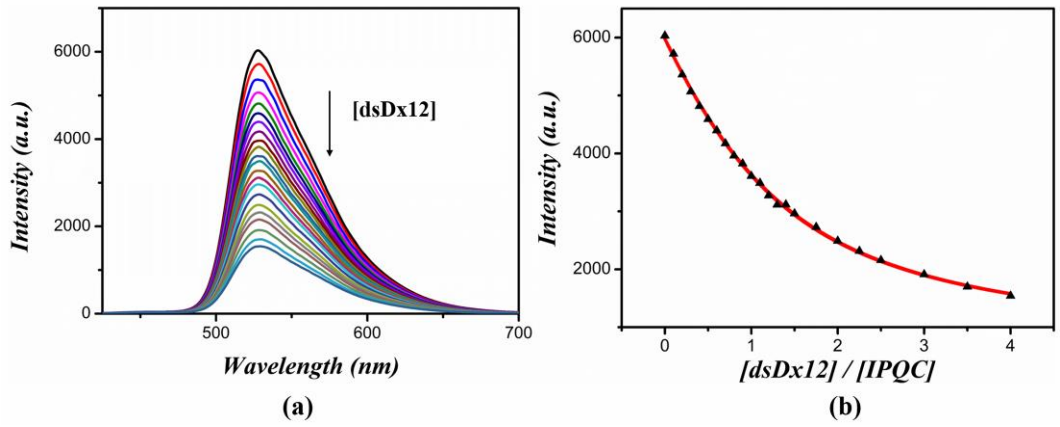

Figure S32 (a) Fluorescence spectroscopic titration of **IPQC** (2.00×10^{-5} M) with dsDx12 (0 to 4.0 molar equiv.); (b) change in the intensity data from 425 nm to 700 nm was used to calculate the $K_{a1} = (6.3 \pm 0.2) \times 10^4$ M^{-1} corresponding to the formation of **IPQC**·dsDx12, using the Hyperquad 2003 program [8]. The red lines show the non-linear curve fit of the experimental data of 528 nm to the appropriate equation. Equations governing the relevant equilibria: $[H] + [G] \overset{K_{a1}}{\rightleftharpoons} [HG]$

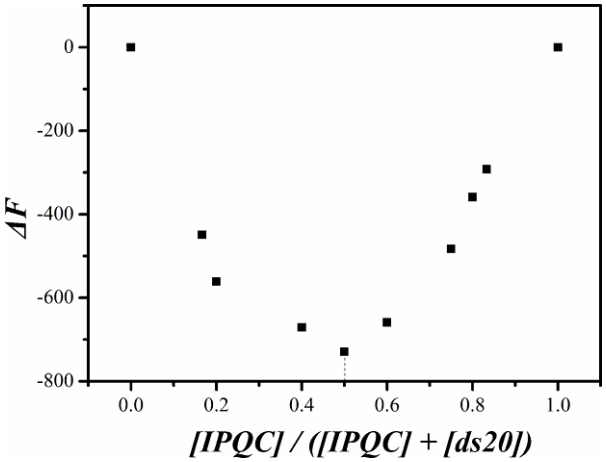

Figure 33 Job-plot corresponding to the interaction between **IPQC** and ds20 at 298 K as monitored via fluorescence spectroscopy. In this study, [**IPQC**] + [ds20] = 2.00 × 10^{-5} M, the minimum value of [**IPQC**] / ([**IPQC**] + [ds20]) was found at 0.5, a finding consistent with a 1:1 (**IPQC**:ds20) binding stoichiometry [7].

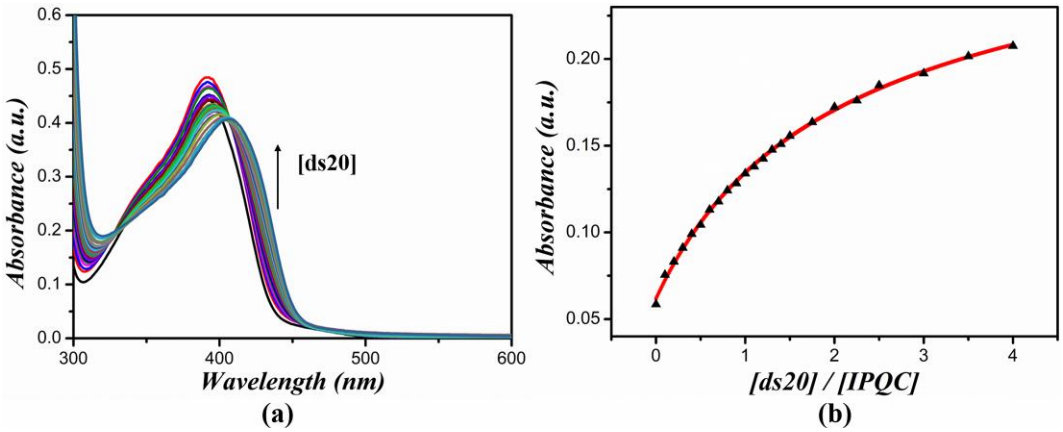

Figure S34 (a) Uv-vis absorption spectroscopic titration of **IPQC** (2.00 × 10^{-5} M) with ds20 (0 to 4.0 molar equiv.); (b) change in the Uv-vis intensity data from 350 nm to 450 nm was used to calculate the K_{a1} = (1.6 ± 0.1) × 10^{4} M^{-1} corresponding to the formation of **IPQC**·ds20, using the Hyperquad 2003 program [8]. The red lines show the non-linear curve fit of the experimental data of 436 nm to the appropriate equation. Equations governing the relevant equilibria: $[H] + [G] \overset{K_{a1}}{\rightleftharpoons} [HG]$

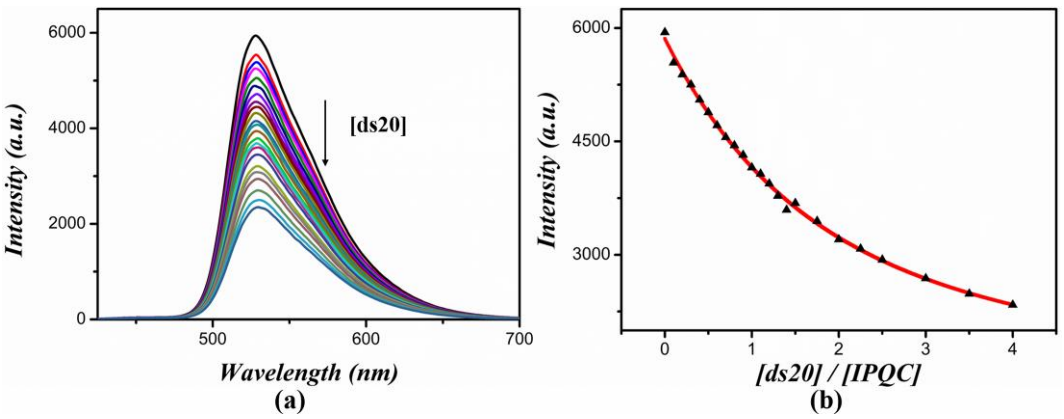

Figure S35 (a) Fluorescence spectroscopic titration of **IPQC** (2.00×10^{-5} M) with ds20 (0 to 4.0 molar equiv.); (b) change in the intensity data from 425 nm to 700 nm was used to calculate the $K_{a1} = (2.0 \pm 0.1) \times 10^4$ M^{-1} corresponding to the formation of **IPQC**·ds20, using the Hyperquad 2003 program [8]. The red lines show the non-linear curve fit of the experimental data of 528 nm to the appropriate equation. Equations governing the relevant equilibria: $[H] + [G] \rightleftharpoons[K_{a1}] [HG]$

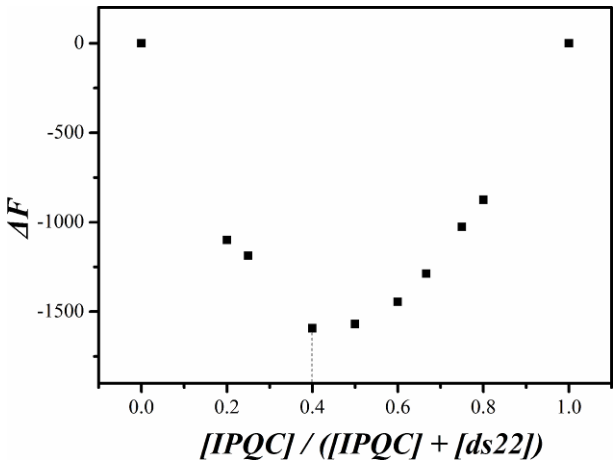

Figure S36 Job-plot corresponding to the interaction between **IPQC** and ds22 at 298 K as monitored via fluorescence spectroscopy. In this study, [**IPQC**] + [ds22] = 2.00×10^{-5} M, the minimum value of [**IPQC**] / ([**IPQC**] + [ds22]) was found at 0.4, a finding consistent with a 2:3 (**IPQC**:ds22) binding stoichiometry [7].

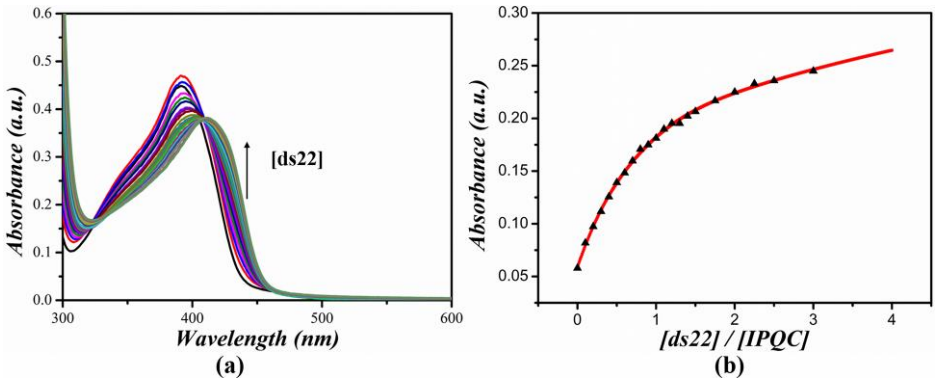

Figure S37 (a) Uv-vis absorption spectroscopic titration of **IPQC** (2.00×10^{-5} M) with ds22 (0 to 4.0 molar equiv.); (b) change in the Uv-vis intensity data from 350 nm to 450 nm was used to calculate the $K_{a1} = (2.0 \pm 0.1) \times 10^5$ M^{-1}, $K_{a2} = (1.6 \pm 0.1) \times 10^4$ M^{-1}, $K_{a3} = (1.3 \pm 0.1) \times 10^6$ M^{-1} corresponding to the formation of **IPQC**·ds22, **IPQC**·$(ds22)_2$, $(\mathbf{IPQC})_2$·$(ds22)_3$, using the Hyperquad 2003 program [8]. The red lines show the non-linear curve fit of the experimental data of 436 nm to the appropriate equation. Equations governing the relevant equilibria: $[H] + [G] \overset{K_{a1}}{\rightleftharpoons} [HG]$ $[HG] + [G] \overset{K_{a2}}{\rightleftharpoons} [HG_2]$ $[HG] + [HG_2] \overset{K_{a3}}{\rightleftharpoons} [H_2G_3]$

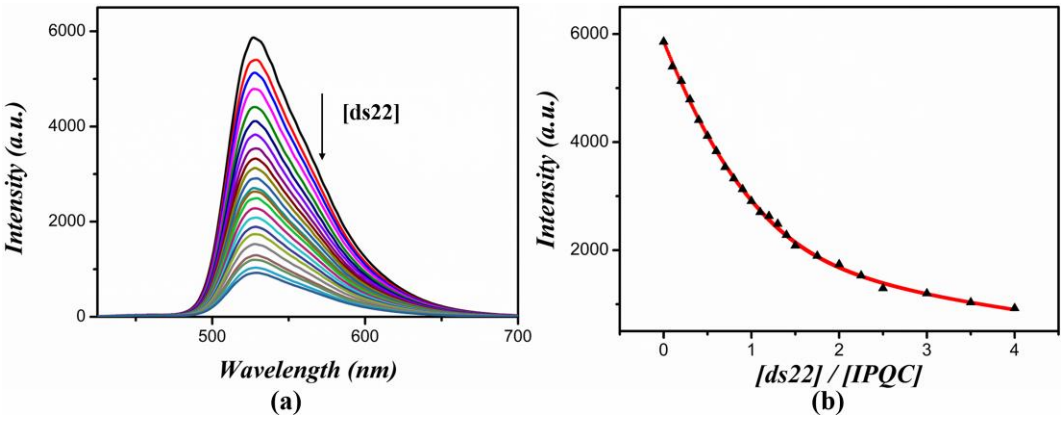

Figure S38 (a) Fluorescence spectroscopic titration of **IPQC** (2.00×10^{-5} M) with ds22 (0 to 4.0 molar equiv.); (b) change in the intensity data from 425 nm to 700 nm was used to calculate the $K_{a1} = (2.0 \pm 0.1) \times 10^5$ M^{-1}, $K_{a2} = (1.3 \pm 0.1) \times 10^4$ M^{-1}, $K_{a3} = (3.2 \pm 0.3) \times 10^5$ M^{-1} corresponding to the formation of **IPQC**·ds22, **IPQC**·$(ds22)_2$, $(\mathbf{IPQC})_2$·$(ds22)_3$, using the Hyperquad 2003 program [8]. The red lines show the non-linear curve fit of the experimental data of 528 nm to the appropriate equation. Equations governing the relevant equilibria: $[H] + [G] \overset{K_{a1}}{\rightleftharpoons} [HG]$ $[HG] + [G] \overset{K_{a2}}{\rightleftharpoons} [HG_2]$ $[HG] + [HG_2] \overset{K_{a3}}{\rightleftharpoons} [H_2G_3]$

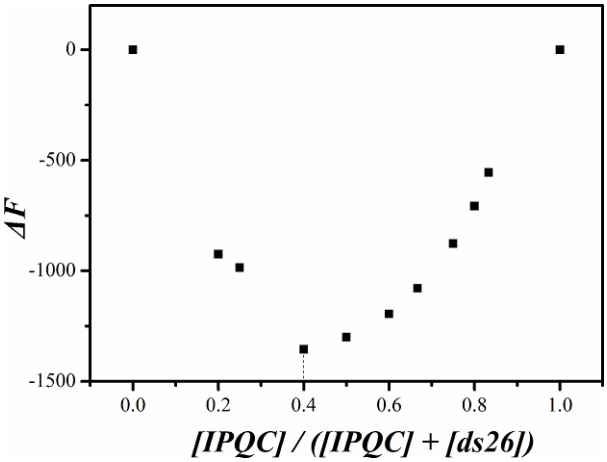

Figure S39 Job-plot corresponding to the interaction between **IPQC** and ds26 at 298 K as monitored via fluorescence spectroscopy. In this study, [**IPQC**] + [ds26] = 2.00 × 10^{-5} M, the minimum value of [**IPQC**] / ([**IPQC**] + [d26]) was found at 0.4, a finding consistent with a 2:3 (**IPQC**:ds26) binding stoichiometry [7].

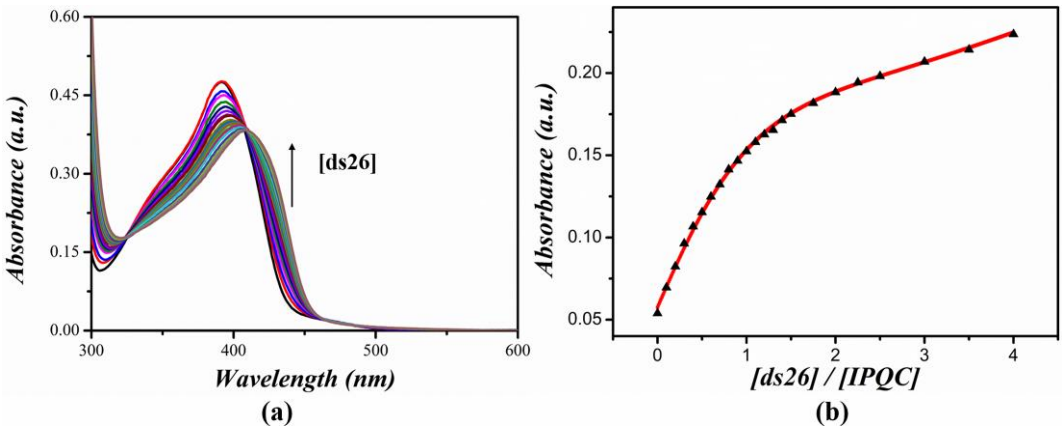

Figure S40 (a) Uv-vis absorption spectroscopic titration of **IPQC** (2.00 × 10^{-5} M) with ds26 (0 to 4.0 molar equiv.); (b) change in the Uv-vis intensity data from 350 nm to 450 nm was used to calculate the K_{a1} = (5.0 ± 0.2) × 10^4 M^{-1}, K_{a2} = (1.0 ± 0.1) × 10^4 M^{-1}, K_{a3} = (7.9 ± 0.6) × 10^4 M^{-1} corresponding to the formation of **IPQC**·ds26, **IPQC**·$(ds26)_2$, $(\mathbf{IPQC})_2$·$(ds26)_3$, using the Hyperquad 2003 program [8]. The red lines show the non-linear curve fit of the experimental data of 436 nm to the appropriate equation. Equations governing the relevant equilibria: $[H] + [G] \overset{K_{a1}}{\rightleftharpoons} [HG]$ $[HG] + [G] \overset{K_{a2}}{\rightleftharpoons} [HG_2]$ $[HG] + [HG_2] \overset{K_{a3}}{\rightleftharpoons} [H_2G_3]$

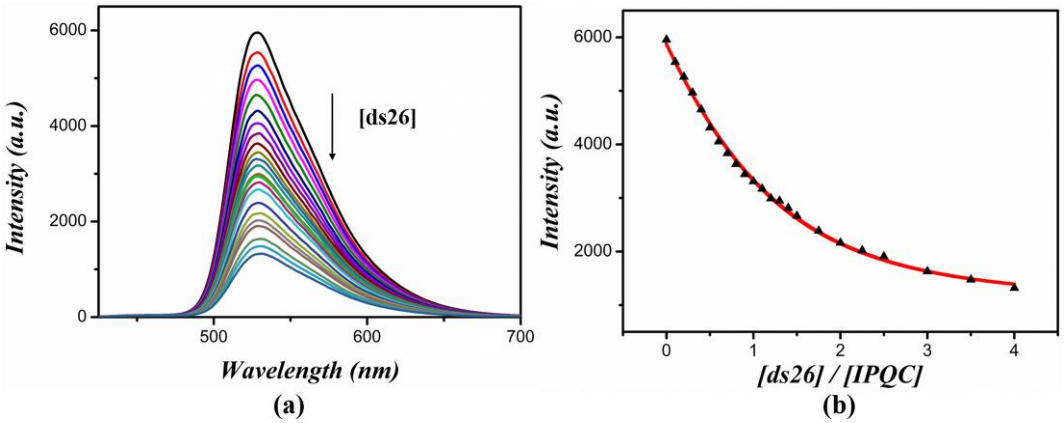

Figure S41 (a) Fluorescence spectroscopic titration of **IPQC** (2.00×10^{-5} M) with ds26 (0 to 4.0 molar equiv.); (b) change in the intensity data from 425 nm to 700 nm was used to calculate the $K_{a1} = (8.0 \pm 0.2) \times 10^4$ M^{-1}, $K_{a2} = (6.3 \pm 0.3) \times 10^3$ M^{-1}, $K_{a3} = (1.6 \pm 0.1) \times 10^4$ M^{-1} corresponding to the formation of **IPQC**·ds26, **IPQC**·$(ds26)_2$, $(\mathbf{IPQC})_2$·$(ds26)_3$, using the Hyperquad 2003 program [8]. The red lines show the non-linear curve fit of the experimental data of 528 nm to the appropriate equation. Equations governing the relevant equilibria: $[H] + [G] \overset{K_{a1}}{\rightleftharpoons} [HG]$ $[HG] + [G] \overset{K_{a2}}{\rightleftharpoons} [HG_2]$ $[HG] + [HG_2] \overset{K_{a3}}{\rightleftharpoons} [H_2G_3]$

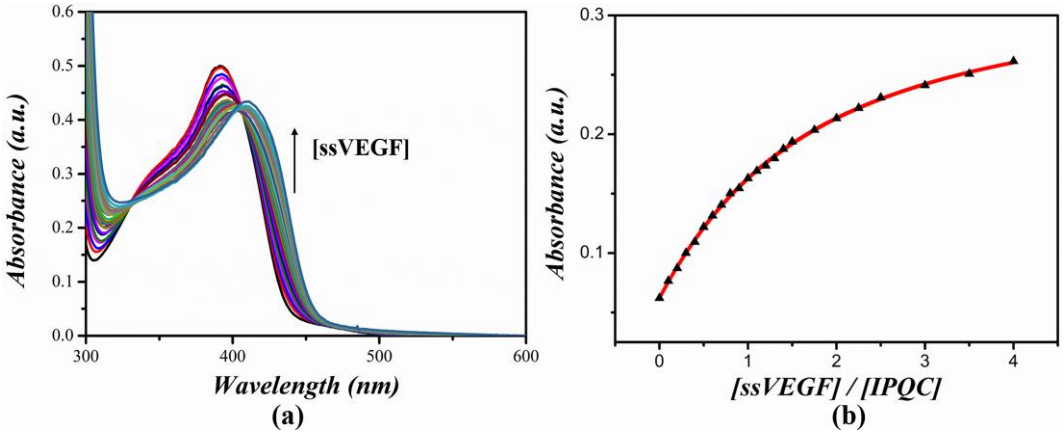

Figure S42 (a) Uv-vis absorption spectroscopic titration of **IPQC** (2.00×10^{-5} M) with ssVEGF (0 to 4.0 molar equiv.); (b) change in the Uv-vis intensity data from 350 nm to 450 nm was used to calculate the $K_{a1} = (5.0 \pm 0.2) \times 10^4$ M^{-1} corresponding to the formation of **IPQC**·ssVEGF, using the Hyperquad 2003 program [8]. The red lines show the non-linear curve fit of the experimental data of 436 nm to the appropriate equation. Equations governing the relevant equilibria: $[H] + [G] \overset{K_{a1}}{\rightleftharpoons} [HG]$

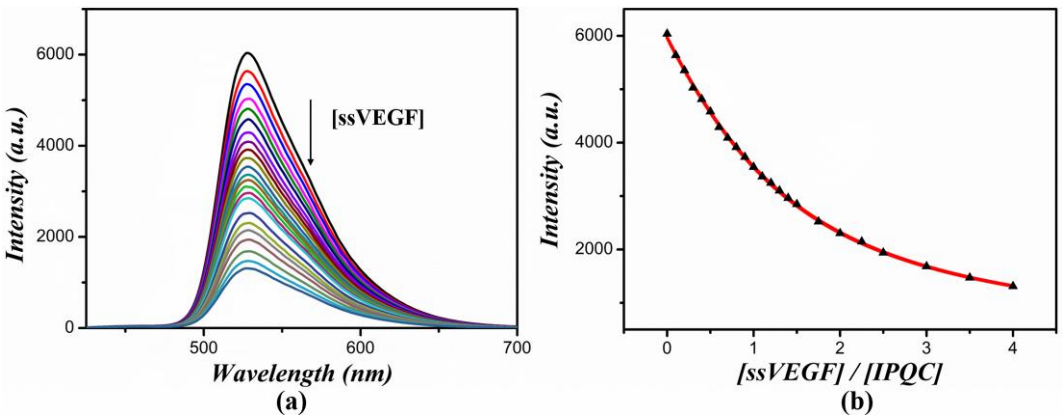

Figure S43 (a) Fluorescence spectroscopic titration of **IPQC** (2.00×10^{-5} M) with ssVEGF (0 to 4.0 molar equiv.); (b) change in the intensity data from 425 nm to 700 nm was used to calculate the $K_{a1} = (6.3 \pm 0.2) \times 10^4$ M^{-1} corresponding to the formation of **IPQC**·ssVEGF, using the Hyperquad 2003 program [8]. The red lines show the non-linear curve fit of the experimental data of 528 nm to the appropriate equation. Equations governing the relevant equilibria: $[H] + [G] \overset{K_{a1}}{\rightleftharpoons} [HG]$

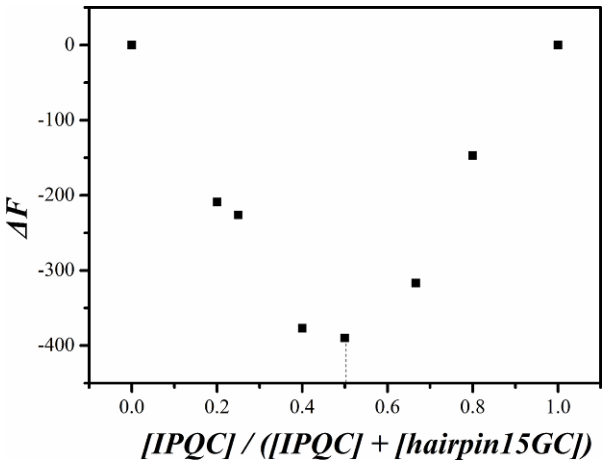

Figure S44 Job-plot corresponding to the interaction between **IPQC** and hairpin15GC at 298 K as monitored via fluorescence spectroscopy. In this study, [**IPQC**] + [hairpin15GC] = 2.00×10^{-5} M, the minimum value of [**IPQC**] / ([**IPQC**] + [hairpin15GC]) was found at 0.5, a finding consistent with a 1:1 (**IPQC**:hairpin15GC) binding stoichiometry [7].

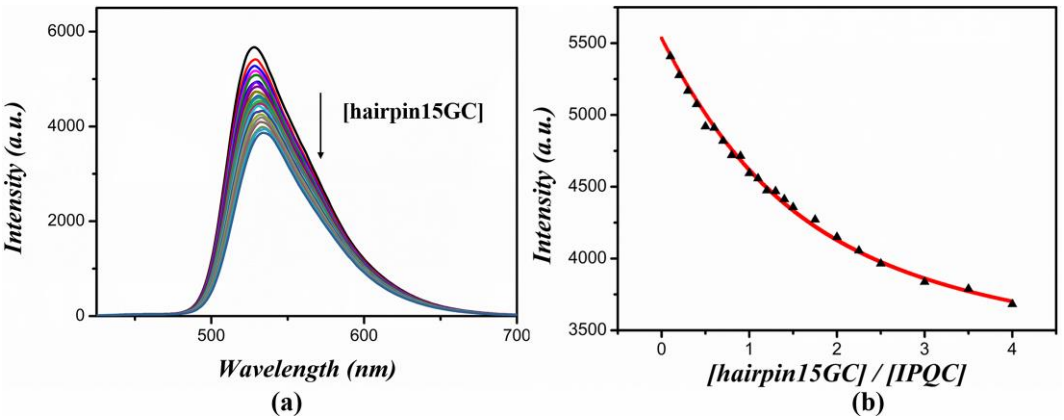

Figure S45 (a) Fluorescence spectroscopic titration of **IPQC** (2.00×10^{-5} M) with hairpin15GC (0 to 4.0 molar equiv.); (b) change in the intensity data from 425 nm to 700 nm was used to calculate the $K_{a1} = (5.0 \pm 0.2) \times 10^4$ M^{-1} corresponding to the formation of **IPQC**·hairpin15GC, using the Hyperquad 2003 program [8]. The red lines show the non-linear curve fit of the experimental data of 528 nm to the appropriate equation. Equations governing the relevant equilibria: $[H] + [G] \overset{K_{a1}}{\rightleftharpoons} [HG]$

∗ Due to weaker response (fluorescence or Uv-vis) between IPQC and partial DNAs (hairpin15GC, ssT30, ssPS1c-a, ssPS1c-b, ssG-tripl, ssAf17), it is unsuccessful to achieve robust quantitative analysis of Uv-vis and fluorescence titration experiment data in these cases.

The complexation study between **IPQC** and G4 DNAs was carried out in the mixture containing ethanol and Tris-HCl buffer ([KCl] = 150 mM, [Tris] = 20 mM; the ratio between ethanol and aqueous phase as 1:99, *v/v*, pH = 7.2).

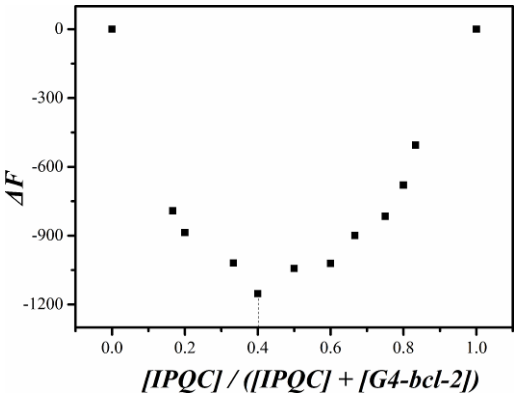

Figure S46 Job-plot corresponding to the interaction between **IPQC** and G4-bcl-2 at 298 K as monitored via fluorescence spectroscopy. In this study, [**IPQC**] + [G4-bcl-2] = 2.00 × 10^{-5} M, the minimum value of [**IPQC**] / ([**IPQC**] + [G4-bcl-2]) was found at 0.4, a finding consistent with a 2:3 (**IPQC**:G4-bcl-2) binding stoichiometry [7].

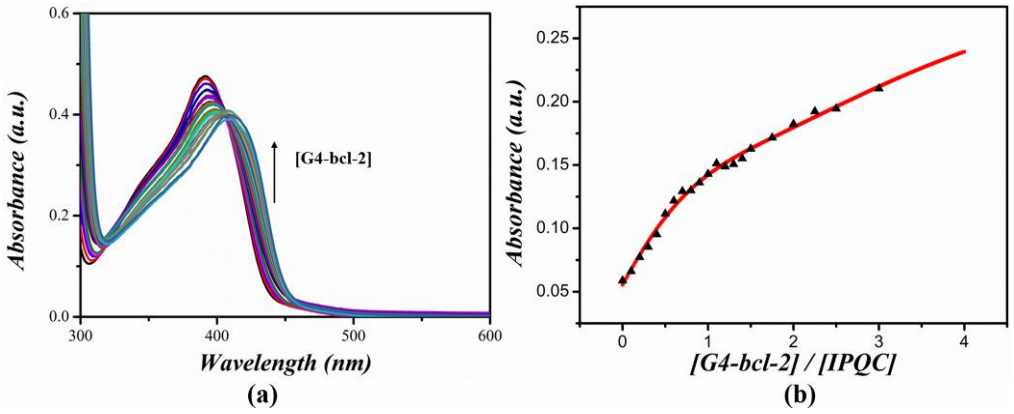

Figure S47 (a) Uv-vis absorption spectroscopic titration of **IPQC** (2.00 × 10^{-5} M) with G4-bcl-2 (0 to 4.0 molar equiv.); (b) change in the Uv-vis intensity data from 350 nm to 450 nm was used to calculate the K_{a1} = (1.6 ± 0.1) × 10^5 M^{-1}, K_{a2} = (5.0 ± 0.3) × 10^4 M^{-1}, K_{a3} = (1.3 ± 0.1) × 10^4 M^{-1} corresponding to the formation of **IPQC**·G4-bcl-2, **IPQC**·**(**G4-bcl-2)$_2$, (**IPQC**)$_2$·**(**G4-bcl-2)$_3$, using the Hyperquad 2003 program [5]. The red lines show the non-linear curve fit of the experimental data of 436 nm to the appropriate equation. Equations governing the relevant equilibria:

$$[H] + [G] \overset{K_{a1}}{\rightleftharpoons} [HG] \quad [HG] + [G] \overset{K_{a2}}{\rightleftharpoons} [HG_2] \quad [HG] + [HG_2] \overset{K_{a3}}{\rightleftharpoons} [H_2G_3]$$

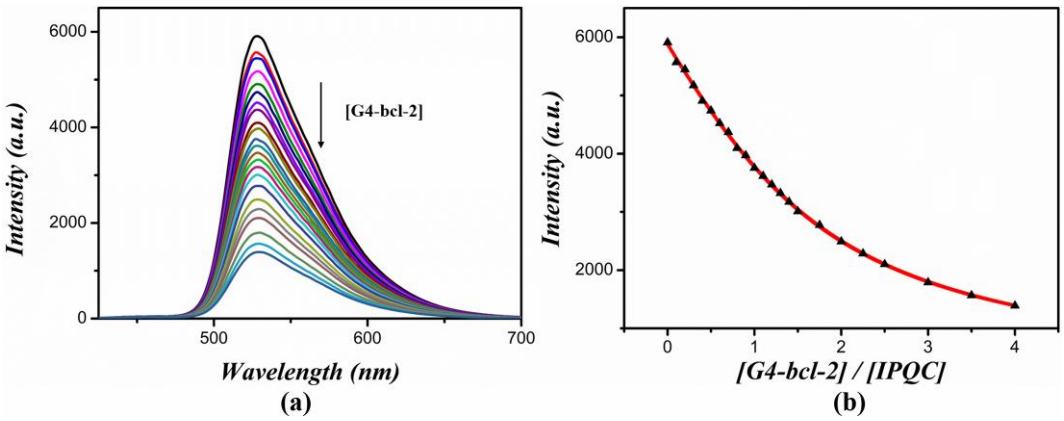

Figure S48 (a) Fluorescence spectroscopic titration of **IPQC** (2.00×10^{-5} M) with G4-bcl-2 (0 to 4.0 molar equiv.); (b) change in the intensity data from 425 nm to 700 nm was used to calculate the $K_{a1} = (2.5 \pm 0.1) \times 10^5$ M^{-1}, $K_{a2} = (2.5 \pm 0.1) \times 10^4$ M^{-1}, $K_{a3} = (4.0 \pm 0.3) \times 10^3$ M^{-1} corresponding to the formation of **IPQC**·G4-bcl-2, **IPQC**·**(**G4-bcl-2)$_2$, (**IPQC**)$_2$·**(**G4-bcl-2)$_3$, using the Hyperquad 2003 program [8]. The red lines show the non-linear curve fit of the experimental data of 528 nm to the appropriate equation. Equations governing the relevant equilibria: $[H] + [G] \overset{K_{a1}}{\rightleftharpoons} [HG]$ $[HG] + [G] \overset{K_{a2}}{\rightleftharpoons} [HG_2]$ $[HG] + [HG_2] \overset{K_{a3}}{\rightleftharpoons} [H_2G_3]$

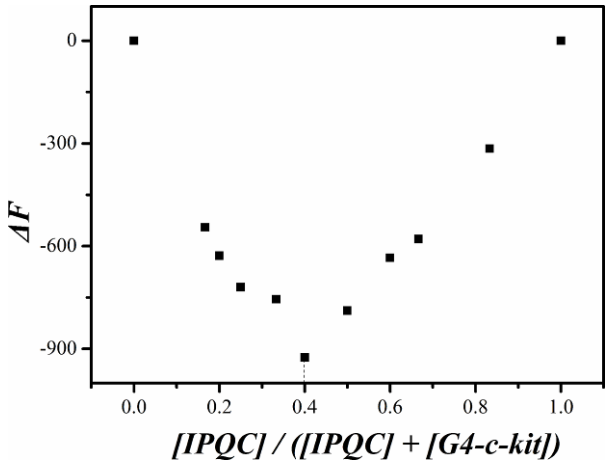

Figure S49 Job-plot corresponding to the interaction between **IPQC** and G4-c-kit at 298 K as monitored via fluorescence spectroscopy. In this study, [**IPQC**] + [G4-c-kit] = 2.00×10^{-5} M, the minimum value of [**IPQC**] / ([**IPQC**] + [G4-c-kit]) was found at 0.4, a finding consistent with a 2:3 (**IPQC**:G4-c-kit) binding stoichiometry [7].

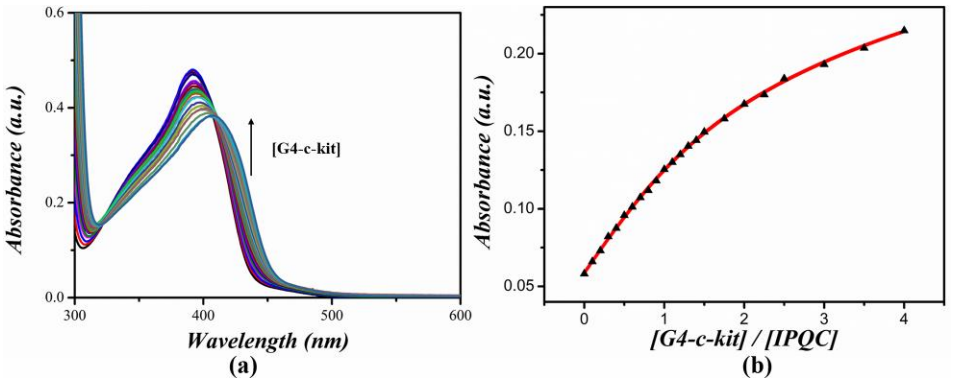

Figure S50 (a) Uv-vis absorption spectroscopic titration of **IPQC** (2.00×10^{-5} M) with G4-c-kit (0 to 4.0 molar equiv.); (b) change in the Uv-vis intensity data from 350 nm to 450 nm was used to calculate the $K_{a1} = (2.0 \pm 0.1) \times 10^5$ M^{-1}, $K_{a2} = (1.6 \pm 0.1) \times 10^4$ M^{-1}, $K_{a3} = (4.0 \pm 0.3) \times 10^4$ M^{-1} corresponding to the formation of **IPQC**·G4-c-kit, **IPQC**·(G4-c-kit)$_2$, (**IPQC**)$_2$·(G4-c-kit)$_3$, using the Hyperquad 2003 program [8]. The red lines show the non-linear curve fit of the experimental data of 436 nm to the appropriate equation. Equations governing the relevant equilibria: $[H] + [G] \overset{K_{a1}}{\rightleftharpoons} [HG]$ $[HG] + [G] \overset{K_{a2}}{\rightleftharpoons} [HG_2]$ $[HG] + [HG_2] \overset{K_{a3}}{\rightleftharpoons} [H_2G_3]$

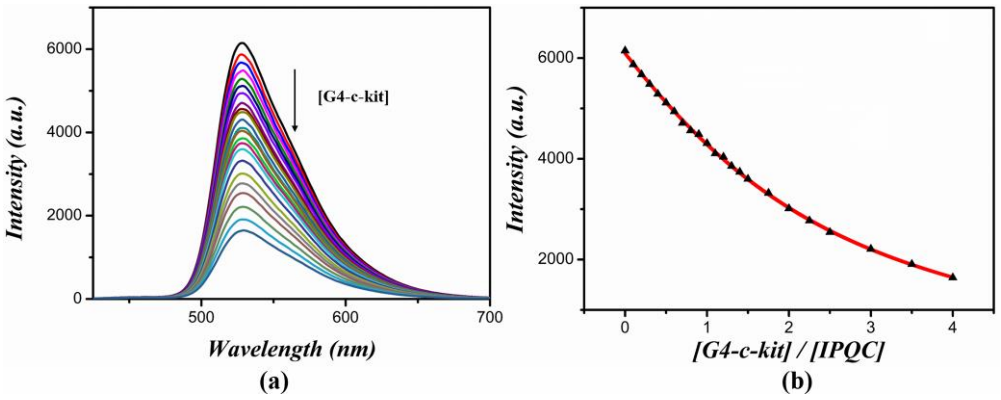

Figure S51 (a) Fluorescence spectroscopic titration of **IPQC** (2.00×10^{-5} M) with G4-c-kit (0 to 4.0 molar equiv.); (b) change in the intensity data from 425 nm to 700 nm was used to calculate the $K_{a1} = (1.3 \pm 0.1) \times 10^5$ M^{-1}, $K_{a2} = (1.6 \pm 0.1) \times 10^4$ M^{-1}, $K_{a3} = (4.0 \pm 0.3) \times 10^3$ M^{-1} corresponding to the formation of **IPQC**·G4-c-kit, **IPQC**·(G4-c-kit)$_2$, (**IPQC**)$_2$·(G4-c-kit)$_3$, using the Hyperquad 2003 program [8]. The red lines show the non-linear curve fit of the experimental data of 528 nm to the appropriate equation. Equations governing the relevant equilibria: $[H] + [G] \overset{K_{a1}}{\rightleftharpoons} [HG]$ $[HG] + [G] \overset{K_{a2}}{\rightleftharpoons} [HG_2]$ $[HG] + [HG_2] \overset{K_{a3}}{\rightleftharpoons} [H_2G_3]$

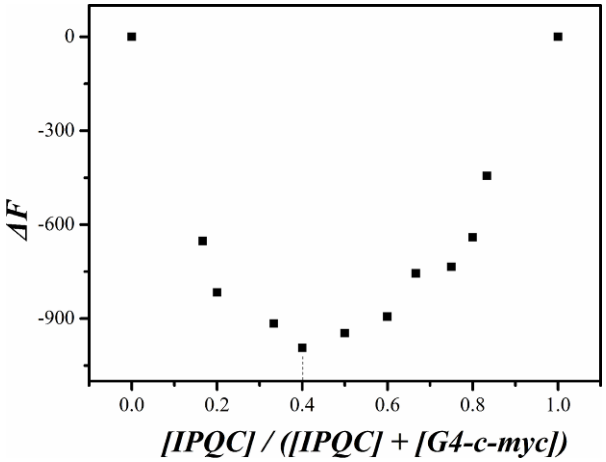

Figure S52 Job-plot corresponding to the interaction between **IPQC** and G4-c-myc at 298 K as monitored via fluorescence spectroscopy. In this study, [**IPQC**] + [G4-c-myc] = 2.00 × 10^{-5} M, the minimum value of [**IPQC**] / ([**IPQC**] + [G4-c-myc]) was found at 0.4, a finding consistent with a 2:3 (**IPQC**:G4-c-myc) binding stoichiometry [7].

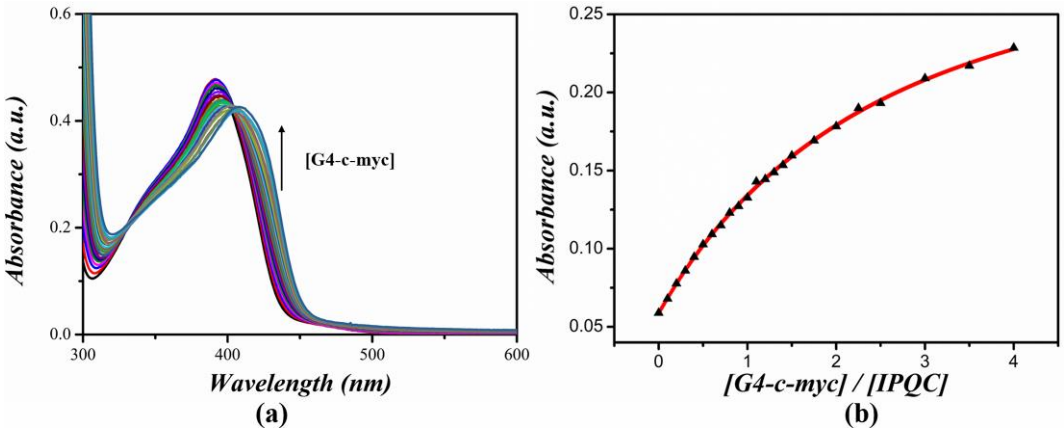

Figure S53 (a) Uv-vis absorption spectroscopic titration of **IPQC** (2.00 × 10^{-5} M) with G4-c-myc (0 to 4.0 molar equiv.); (b) change in the Uv-vis intensity data from 350 nm to 450 nm was used to calculate the K_{a1} = (1.6 ± 0.1) × 10^5 M^{-1}, K_{a2} = (6.3 ± 0.3) × 10^4 M^{-1}, K_{a3} = (1.0 ± 0.1) × 10^5 M^{-1} corresponding to the formation of **IPQC**·G4-c-myc, **IPQC**·**(**G4-c-myc)$_2$, (**IPQC**)$_2$·**(**G4-c-myc)$_3$, using the Hyperquad 2003 program [8]. The red lines show the non-linear curve fit of the experimental data of 436 nm to the appropriate equation. Equations governing the relevant equilibria:

$$[H] + [G] \overset{K_{a1}}{\rightleftharpoons} [HG] \quad [HG] + [G] \overset{K_{a2}}{\rightleftharpoons} [HG_2] \quad [HG] + [HG_2] \overset{K_{a3}}{\rightleftharpoons} [H_2G_3]$$

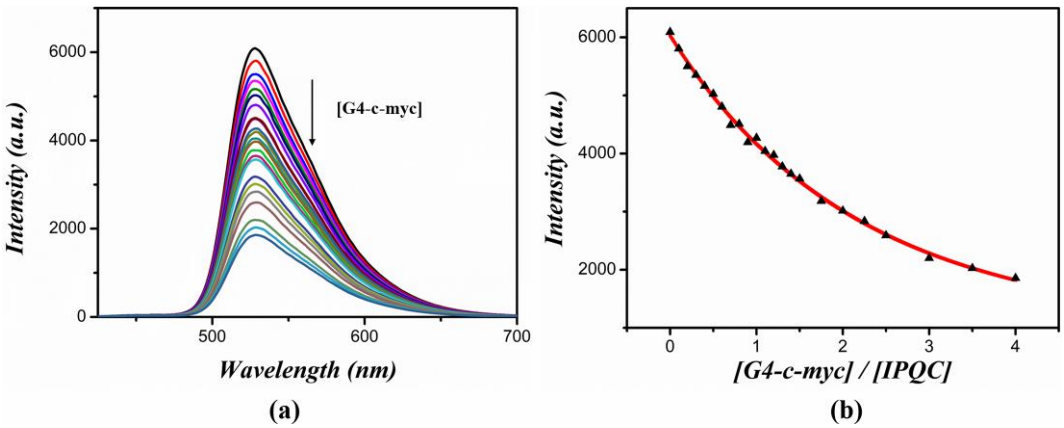

Figure S54 (a) Fluorescence spectroscopic titration of **IPQC** (2.00×10^{-5} M) with G4-c-myc (0 to 4.0 molar equiv.); (b) change in the intensity data from 425 nm to 700 nm was used to calculate the $K_{a1} = (5.0 \pm 0.2) \times 10^4$ M^{-1}, $K_{a2} = (7.9 \pm 0.4) \times 10^4$ M^{-1}, $K_{a3} = (5.0 \pm 0.4) \times 10^4$ M^{-1} corresponding to the formation of **IPQC**·G4-c-myc, **IPQC**·(G4-c-myc)$_2$, (**IPQC**)$_2$·(G4-c-myc)$_3$, using the Hyperquad 2003 program [8]. The red lines show the non-linear curve fit of the experimental data of 528 nm to the appropriate equation. Equations governing the relevant equilibria: $[H] + [G] \overset{K_{a1}}{\rightleftharpoons} [HG]$ $[HG] + [G] \overset{K_{a2}}{\rightleftharpoons} [HG_2]$ $[HG] + [HG_2] \overset{K_{a3}}{\rightleftharpoons} [H_2G_3]$

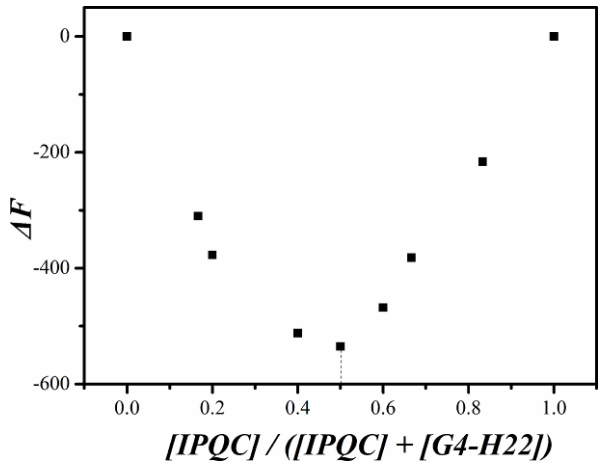

Figure S55 Job-plot corresponding to the interaction between **IPQC** and G4-H22 at 298 K as monitored via fluorescence spectroscopy. In this study, [**IPQC**] + [G4-H22] = 2.00×10^{-5} M, the minimum value of [**IPQC**] / ([**IPQC**] + [G4-H22]) was found at 0.5, a finding consistent with a 1:1 (**IPQC**:G4-H22) binding stoichiometry [7].

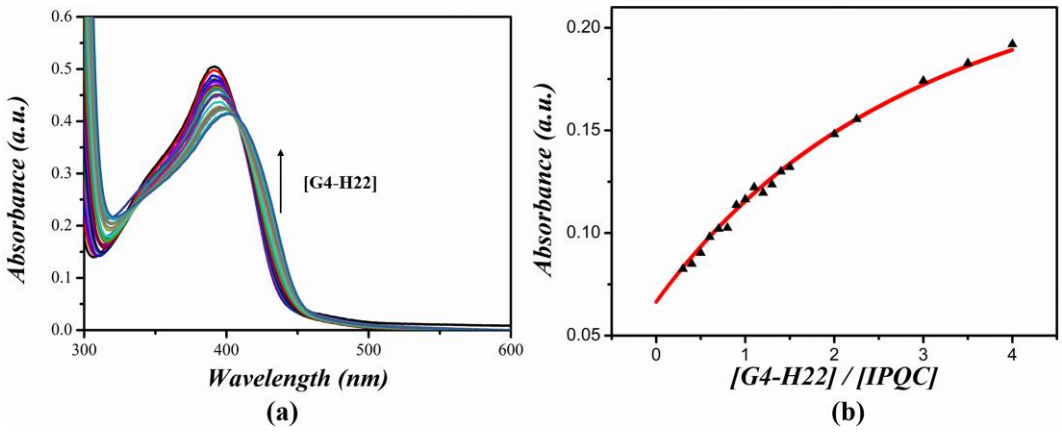

Figure S56 (a) Uv-vis absorption spectroscopic titration of **IPQC** (2.00×10^{-5} M) with G4-H22 (0 to 4.0 molar equiv.); (b) change in the Uv-vis intensity data from 350 nm to 450 nm was used to calculate the $K_{a1} = (2.0 \pm 0.1) \times 10^4$ M^{-1} corresponding to the formation of **IPQC**·G4-H22, using the Hyperquad 2003 program [8]. The red lines show the non-linear curve fit of the experimental data of 436 nm to the appropriate equation. Equations governing the relevant equilibria: $[H] + [G] \overset{K_{a1}}{\rightleftharpoons} [HG]$

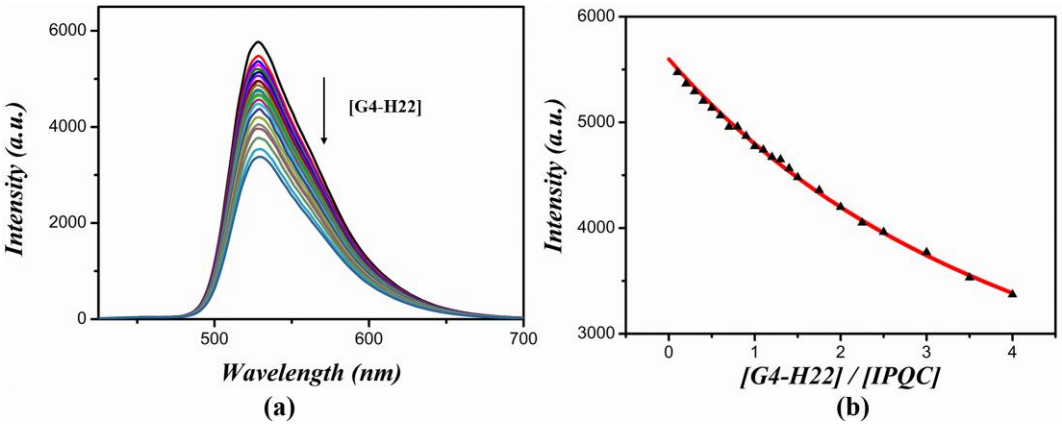

Figure S57 (a) Fluorescence spectroscopic titration of **IPQC** (2.00×10^{-5} M) with G4-H22 (0 to 4.0 molar equiv.); (b) change in the intensity data from 425 nm to 700 nm was used to calculate the $K_{a1} = (1.3 \pm 0.1) \times 10^4$ M^{-1} corresponding to the formation of **IPQC**·G4-H22, using the Hyperquad 2003 program [8]. The red lines show the non-linear curve fit of the experimental data of 528 nm to the appropriate equation. Equations governing the relevant equilibria: $[H] + [G] \overset{K_{a1}}{\rightleftharpoons} [HG]$

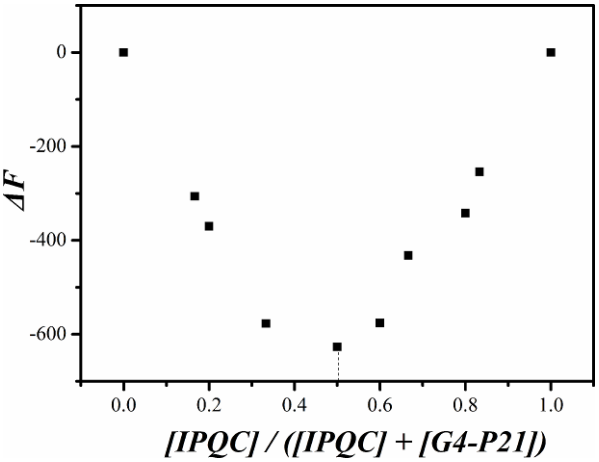

Figure S58 Job-plot corresponding to the interaction between **IPQC** and G4-P21 at 298 K as monitored via fluorescence spectroscopy. In this study, [**IPQC**] + [G4-P21] = 2.00 × 10^{-5} M, the minimum value of [**IPQC**] / ([**IPQC**] + [G4-P21]) was found at 0.5, a finding consistent with a 1:1 (**IPQC**:G4-P21) binding stoichiometry [7].

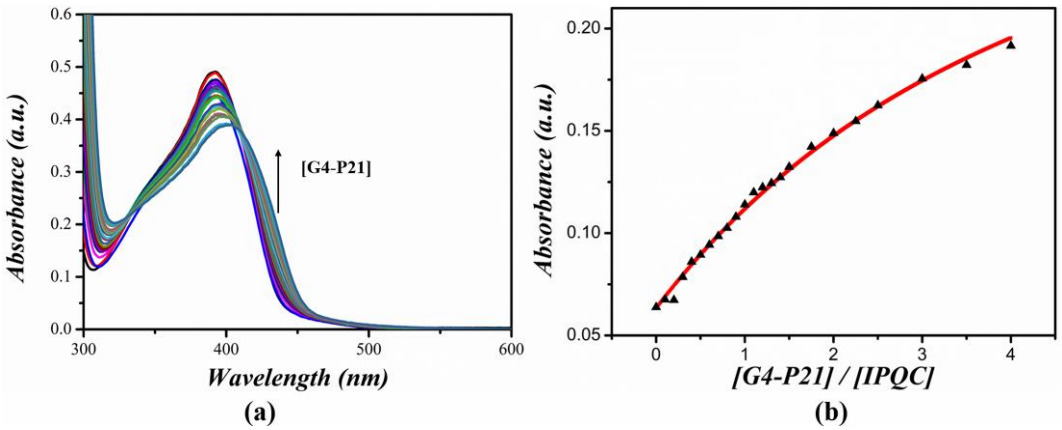

Figure S59 (a) Uv-vis absorption spectroscopic titration of **IPQC** (2.00 × 10^{-5} M) with G4-P21 (0 to 4.0 molar equiv.); (b) change in the Uv-vis intensity data from 350 nm to 450 nm was used to calculate the K_{a1} = (1.3 ± 0.1) × 10^{4} M^{-1} corresponding to the formation of **IPQC**·G4-P21, using the Hyperquad 2003 program [8]. The red lines show the non-linear curve fit of the experimental data of 436 nm to the appropriate equation. Equations governing the relevant equilibria: $[H] + [G] \overset{K_{a1}}{\rightleftharpoons} [HG]$

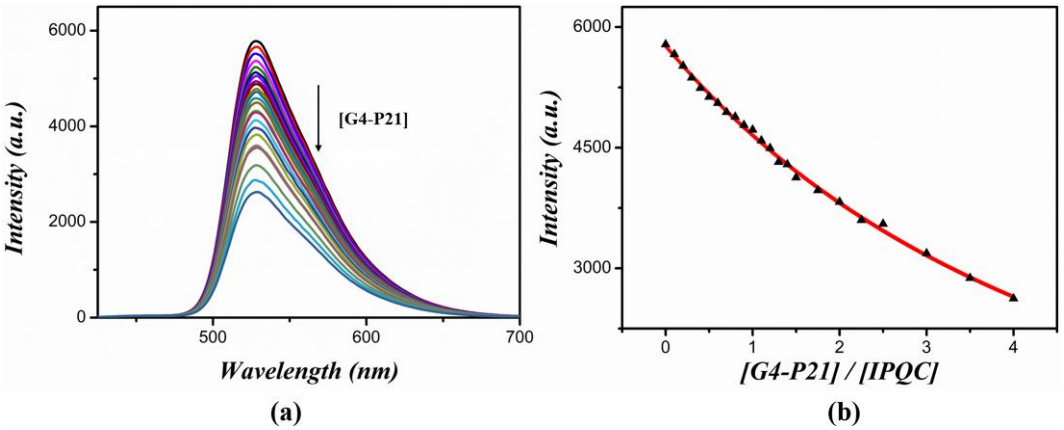

Figure S60 (a) Fluorescence spectroscopic titration of **IPQC** (2.00×10^{-5} M) with G4-P21 (0 to 4.0 molar equiv.); (b) change in the intensity data from 425 nm to 700 nm was used to calculate the K_{a1} = (1.0 ± 0.1) × 10^4 M^{-1} corresponding to the formation of **IPQC**·G4-P21, using the Hyperquad 2003 program [8]. The red lines show the non-linear curve fit of the experimental data of 528 nm to the appropriate equation. Equations governing the relevant equilibria: $[H] + [G] \overset{K_{a1}}{\rightleftharpoons} [HG]$

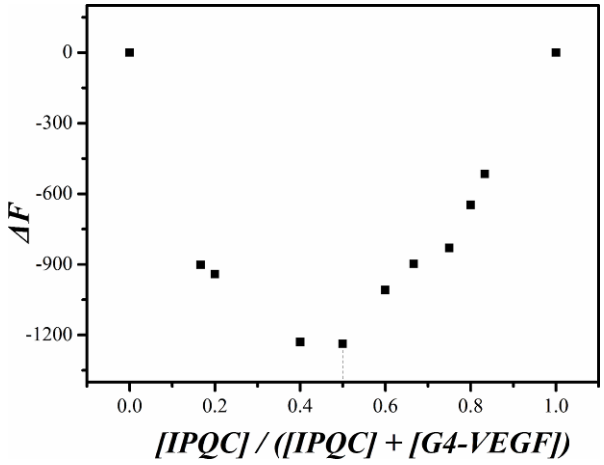

Figure S61 Job-plot corresponding to the interaction between **IPQC** and G4-VEGF at 298 K as monitored via fluorescence spectroscopy. In this study, [**IPQC**] + [G4-VEGF] = 2.00×10^{-5} M, the minimum value of [**IPQC**] / ([**IPQC**] + [G4-VEGF]) was found at 0.5, a finding consistent with a 1:1 (**IPQC**:G4-VEGF) binding stoichiometry [7].

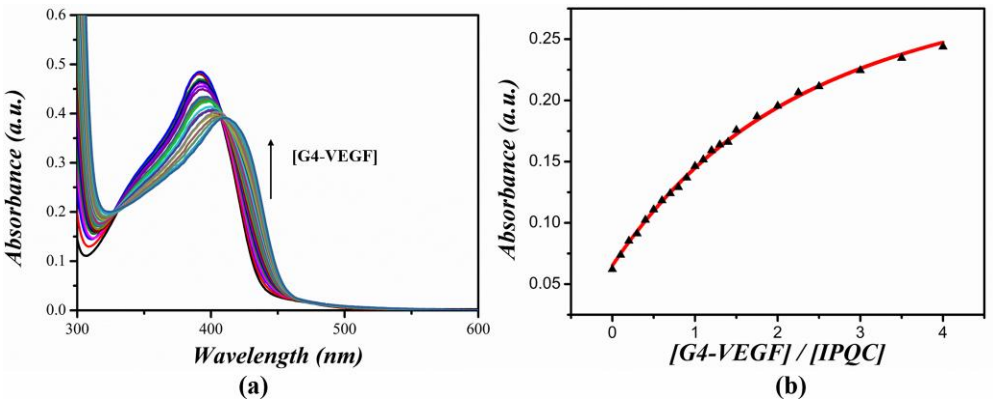

Figure S62 (a) Uv-vis absorption spectroscopic titration of **IPQC** (2.00×10^{-5} M) with G4-VEGF (0 to 4.0 molar equiv.); (b) change in the Uv-vis intensity data from 350 nm to 450 nm was used to calculate the $K_{a1} = (2.5 \pm 0.1) \times 10^4$ M^{-1} corresponding to the formation of **IPQC**·G4-VEGF, using the Hyperquad 2003 program [8]. The red lines show the non-linear curve fit of the experimental data of 436 nm to the appropriate equation. Equations governing the relevant equilibria: $[H] + [G] \overset{K_{a1}}{\rightleftharpoons} [HG]$

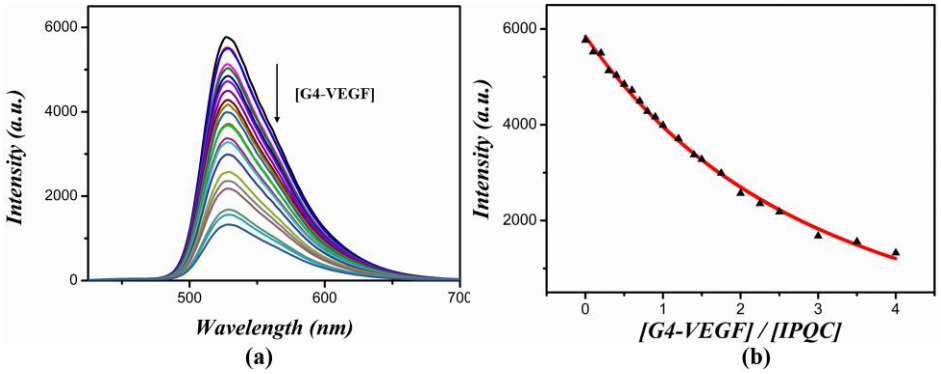

Figure S63 (a) Fluorescence spectroscopic titration of **IPQC** (2.00×10^{-5} M) with G4-VEGF (0 to 4.0 molar equiv.); (b) change in the intensity data from 425 nm to 700 nm was used to calculate the $K_{a1} = (2.0 \pm 0.1) \times 10^4$ M^{-1} corresponding to the formation of **IPQC**·G4-VEGF, using the Hyperquad 2003 program [8]. The red lines show the non-linear curve fit of the experimental data of 528 nm to the appropriate equation. Equations governing the relevant equilibria: $[H] + [G] \overset{K_{a1}}{\rightleftharpoons} [HG]$

∗ Due to weaker response (fluorescence or Uv-vis) between IPQC and ss/ds DNAs in high [K^+] environment, it is unsuccessful to achieve robust quantitative analysis from experiment data in these cases.

Section S6: The molecular simulation

All of the DNA structures were built by the "Build and Edit Nucleic Acid" module of the Discovery Studio software package or retrived from RCSB PDB. The structure of ssVEGF (single stranded DNA) was built as "DNA-single strand" mode. The structure of ds22 (double stranded DNA) was built as "DNA-double strand (A-helix)" mode. The structure of G4-H22 was retrived from RCSB PDB (PDB code: 3T5E). The structure of G4-VEGF was generated by mutating nucleotides from the c-MYC G4 (PDB code: 2L7V) as the VEGF G4 and c-MYC G4 are both parallel G4 and show very similar circular dichroism patterns. The **IPQC** molecule was docked to the DNA structures at different sites and only the **IPQC**-DNA structures with lowest energy were retained.

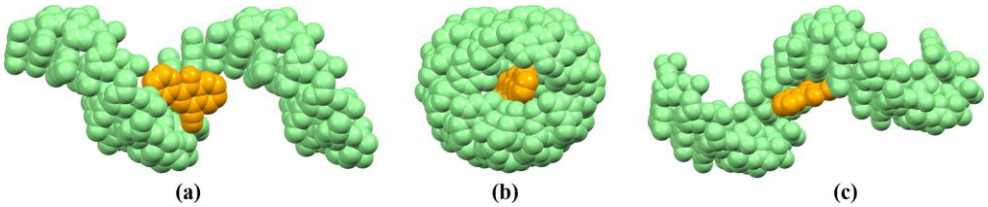

Figure S64 The top (a), side (b) and front (c) views of the optimal structure of 1:1 complexation between ssVEGF (light green) and **IPQC** (orange) are shown as molecular surface.

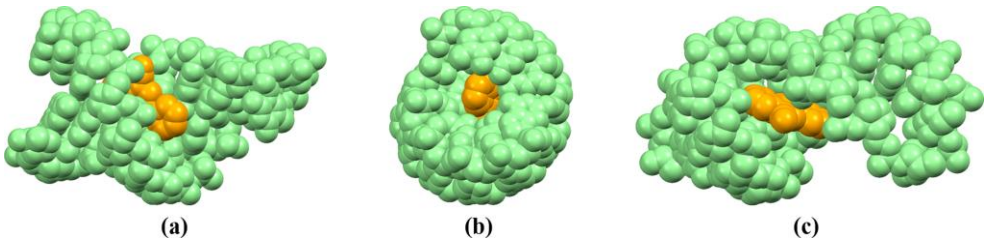

Figure S65 The top (a), side (b) and front (c) views of the optimal structure of 1:1 complexation between ds22 (light green) and **IPQC** (orange) are shown as molecular surface.

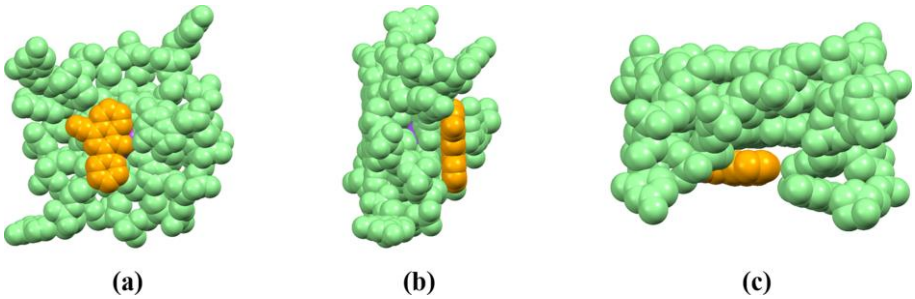

Figure S66 The top (a), side (b) and front (c) views of the optimal structure of 1:1 complexation between G4 VEGF (light green) and **IPQC** (orange) are shown as molecular surface.

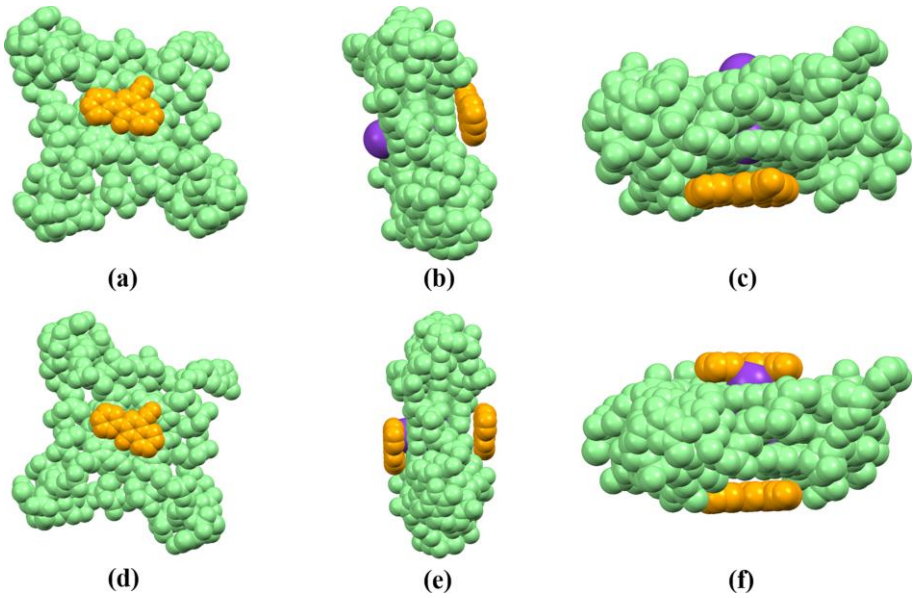

Figure S67 The top (a), side (b) and front (c) views of the optimal structure of 1:1 complexation and the top (d), side (e) and front (f) views of the optimal structure of 1:2 complexation between G4-H22 (light green) and **IPQC** (orange) are shown as molecular surface.

Section S7: **Adduct effect study.**

pH dependent fluorescence and G4-VEGF binding study of **IPQC**.

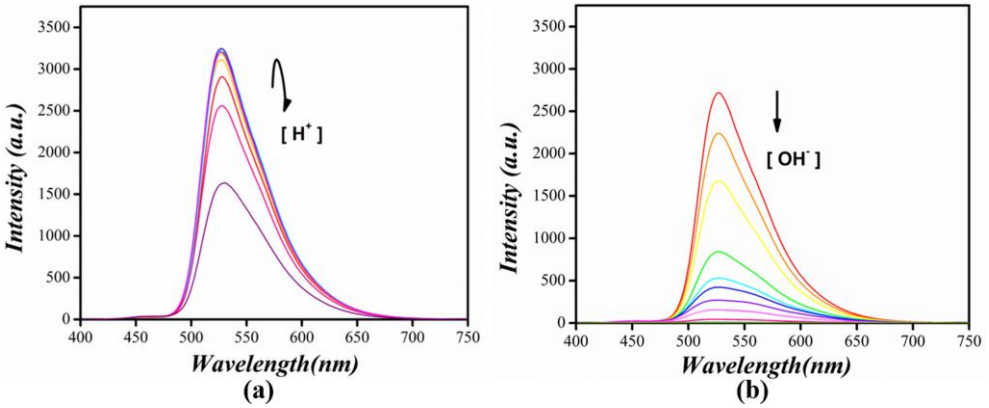

Figure S68 (a) Fluorescence spectroscopic titration of **IPQC** (2.00×10^{-5} M) with increasing concentration of HCl; (b) fluorescence spectroscopic titration of **IPQC** (2.00×10^{-5} M) with increasing concentration of $Me_4N^+OH^-$.

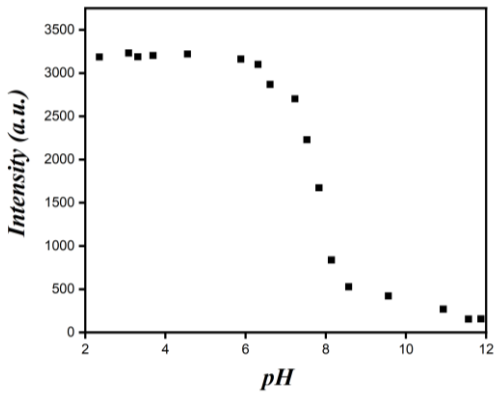

Figure S69 pH dependent fluorescence intensity from 425 nm to 700 nm of **IPQC** (2.00×10^{-5} M).

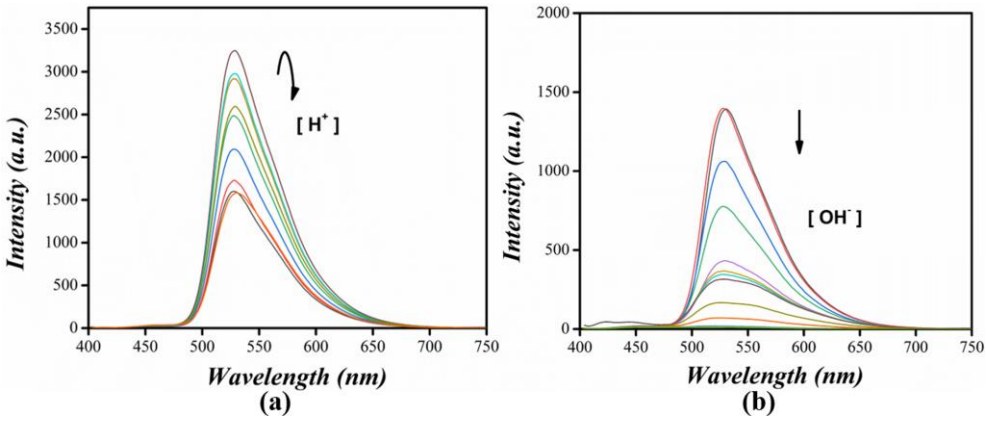

Figure S70 (a) Fluorescence spectroscopic titration of the mixture of 1 equiv. **IPQC** (2.00×10^{-5} M) and 1 equiv. G4-VEGF with increasing concentration of HCl; (b) fluorescence spectroscopic titration of the mixture of **IPQC** (2.00×10^{-5} M) and 1 molar equiv. G4-VEGF with increasing concentration of $Me_4N^+OH^-$.

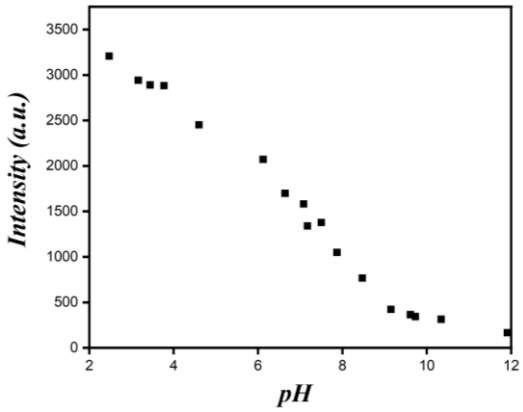

Figure S71 pH dependent fluorescence intensity from 425 nm to 700 nm of the mixture containing **IPQC** (2.00×10^{-5} M) and 1 molar equiv. of G4-VEGF.

CD spectra study was carried out to detect the effect of additional **IPQC** on DNA conformation.

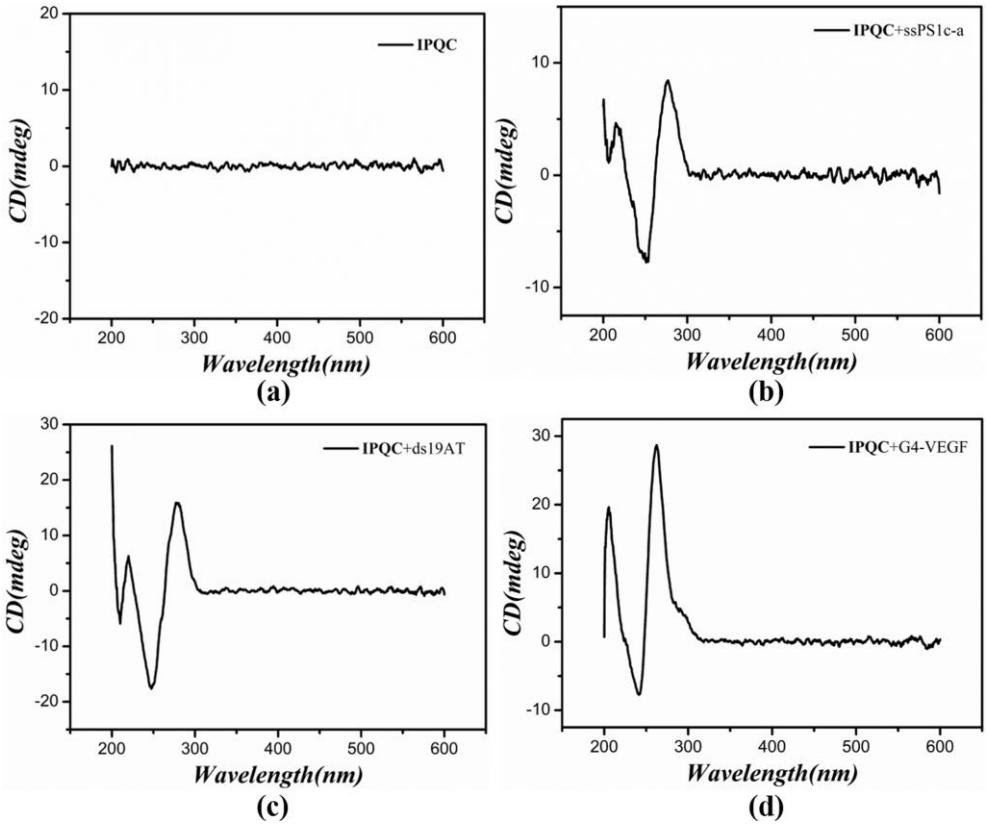

Figure S72 CD (circular dichroism) spectra of a: **IPQC**, b: **IPQC**+ssPS1c-a, c: **IPQC** +G4-VEGF (2.00×10^{-5} M) in the mixture containing ethanol and Tris-HCl buffer ([Tris] = 20 mM; the ratio between ethanol and aqueous phase as 1:99, *v/v*, pH = 7.2, KCl (150 mM) added for G4-VEGF), indicating **IPQC** has no chirality in the long-wave direction.

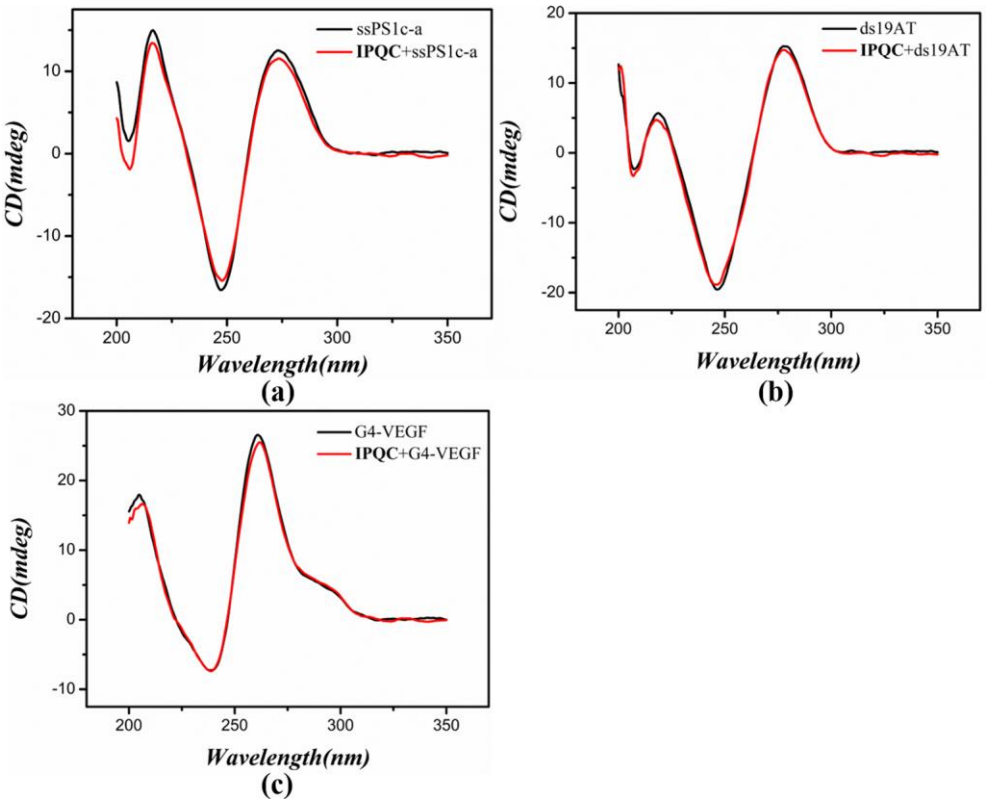

Figure S73 CD (circular dichroism) spectra of a: ssPS1c-a, b: ds19AT, c: G4-VEGF (2.00×10^{-5} M) in the presence or absence of 1.0 molar equiv. of **IPQC** in the mixture containing ethanol and Tris-HCl buffer ([Tris] = 20 mM; the ratio between ethanol and aqueous phase as 1:99, *v/v*, pH = 7.2, KCl (150 mM) added for G4-VEGF), indicating **IPQC** do no affect DNA's structures.

Effects of more additional other cations (Na^+ and Mg^{2+}) in simulated intracellular fluid in the interaction between **IPQC** and DNA.

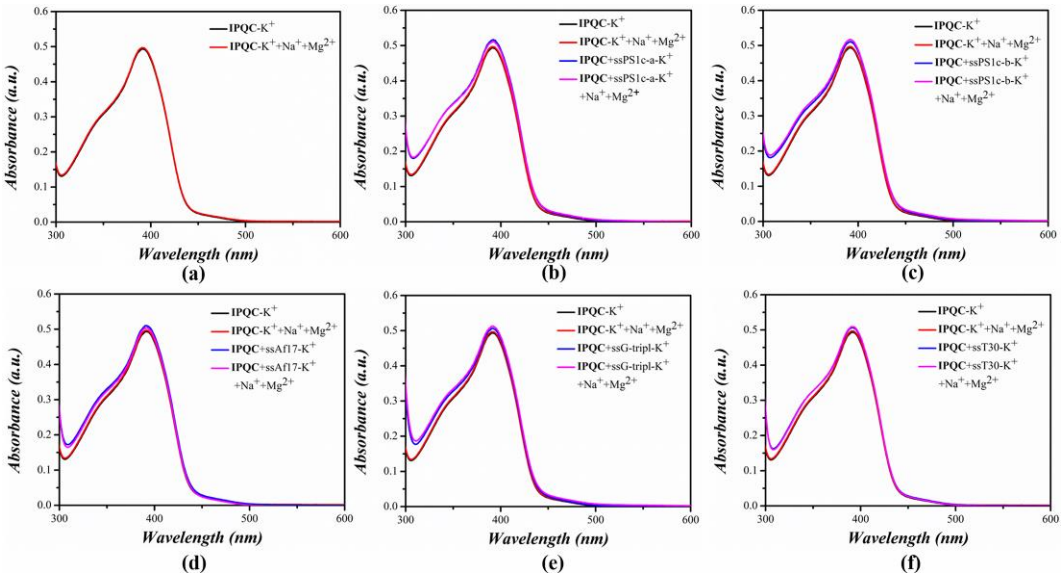

Figure S74 Uv-vis spectra of **IPQC** (2.00×10^{-5} M) with various ssDNAs (2.00×10^{-5} M) adding in the presence or absence of 20 mM Mg^{2+} ($MgCl_2$) and 10 mM Na^+ (NaCl) in the mixture containing ethanol and Tris-HCl buffer ([KCl] = 150 mM; [Tris] = 20 mM; the ratio between ethanol and aqueous phase as 1:99, *v/v*, pH = 7.2).

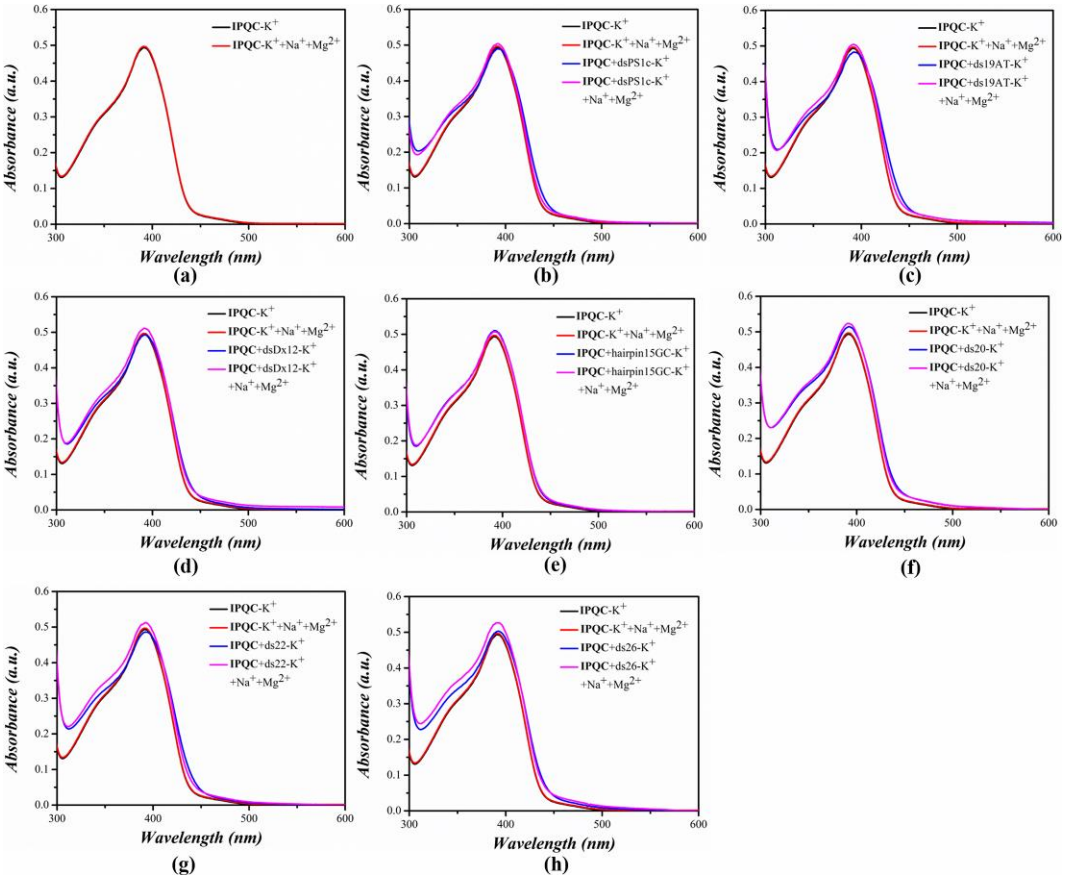

Figure S75 Uv-vis spectra of **IPQC** (2.00×10^{-5} M) with various dsDNAs (2.00×10^{-5} M) adding in the presence or absence of 20 mM Mg^{2+} ($MgCl_2$) and 10 mM Na^+ (NaCl) in the mixture containing ethanol and Tris-HCl buffer ([KCl] = 150 mM; [Tris] = 20 mM; the ratio between ethanol and aqueous phase as 1:99, *v/v*, pH = 7.2).

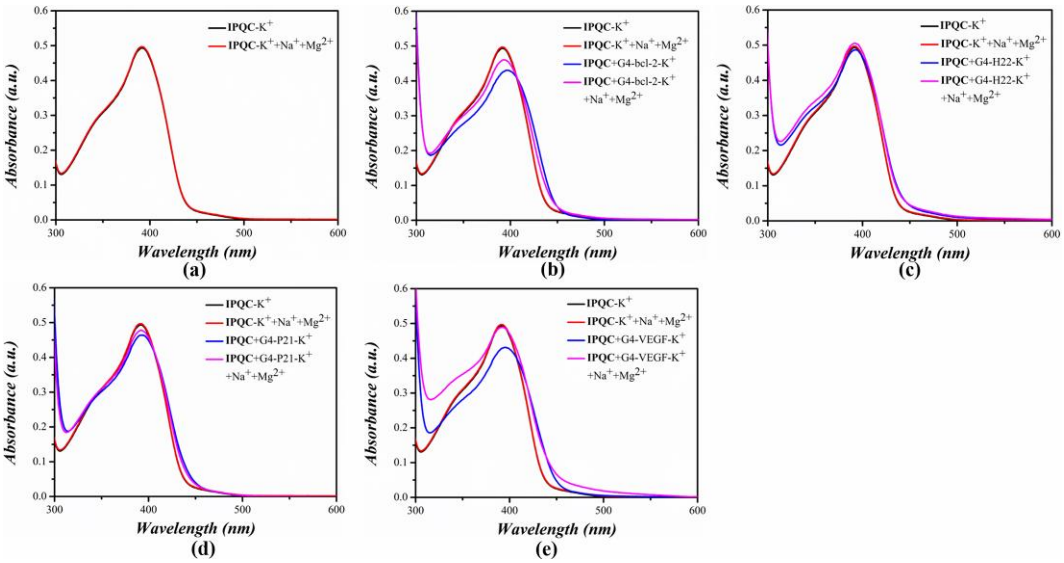

Figure S76 Uv-vis spectra of **IPQC** (2.00×10^{-5} M) with various G4 DNAs (2.00×10^{-5} M) adding in the presence or absence of 20 mM Mg^{2+} ($MgCl_2$) and 10 mM Na^+ (NaCl) in the mixture containing ethanol and Tris-HCl buffer ([KCl] = 150 mM; [Tris] = 20 mM; the ratio between ethanol and aqueous phase as 1:99, *v/v*, pH = 7.2).

∗ It has been reported that magnesium ions may interact with c-kit [9], therefore, we failed to obtain the normal Uv-vis absorption spectrum for evaluating the effects of magnesium ions, same as c-myc.

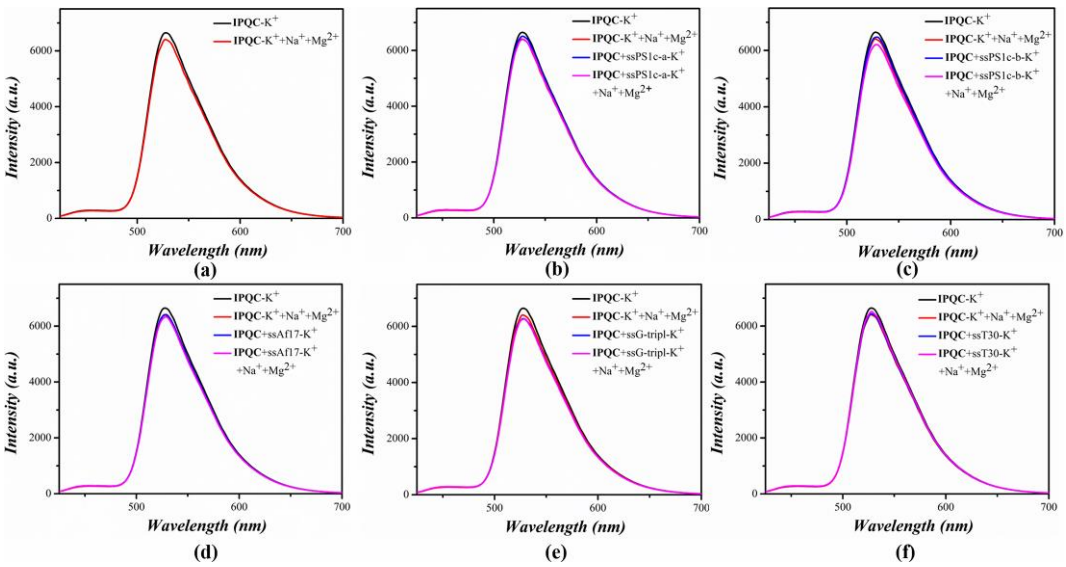

Figure S77 Fluorescence spectra of **IPQC** (2.00×10^{-5} M) with various ssDNAs (2.00×10^{-5} M) adding in the presence or absence of 20 mM Mg^{2+} ($MgCl_2$) and 10 mM Na^+ (NaCl) in the mixture containing ethanol and Tris-HCl buffer ([KCl] = 150 mM; [Tris] = 20 mM; the ratio between ethanol and aqueous phase as 1:99, *v/v*, pH = 7.2).

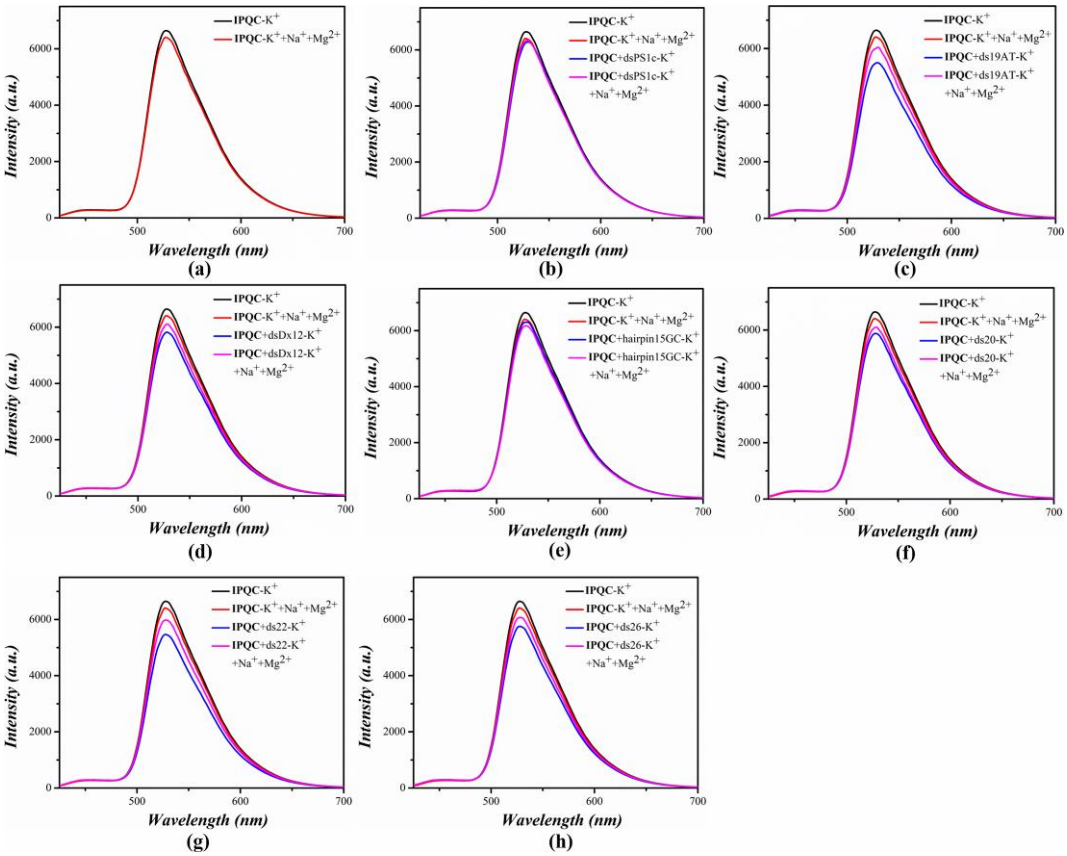

Figure S78 Fluorescence spectra of **IPQC** (2.00×10^{-5} M) with various dsDNAs (2.00×10^{-5} M) adding in the presence or absence of 20 mM Mg^{2+} ($MgCl_2$) and 10

mM Na^+ (NaCl) in the mixture containing ethanol and Tris-HCl buffer ([KCl] = 150 mM; [Tris] = 20 mM; the ratio between ethanol and aqueous phase as 1:99, *v/v*, pH = 7.2).

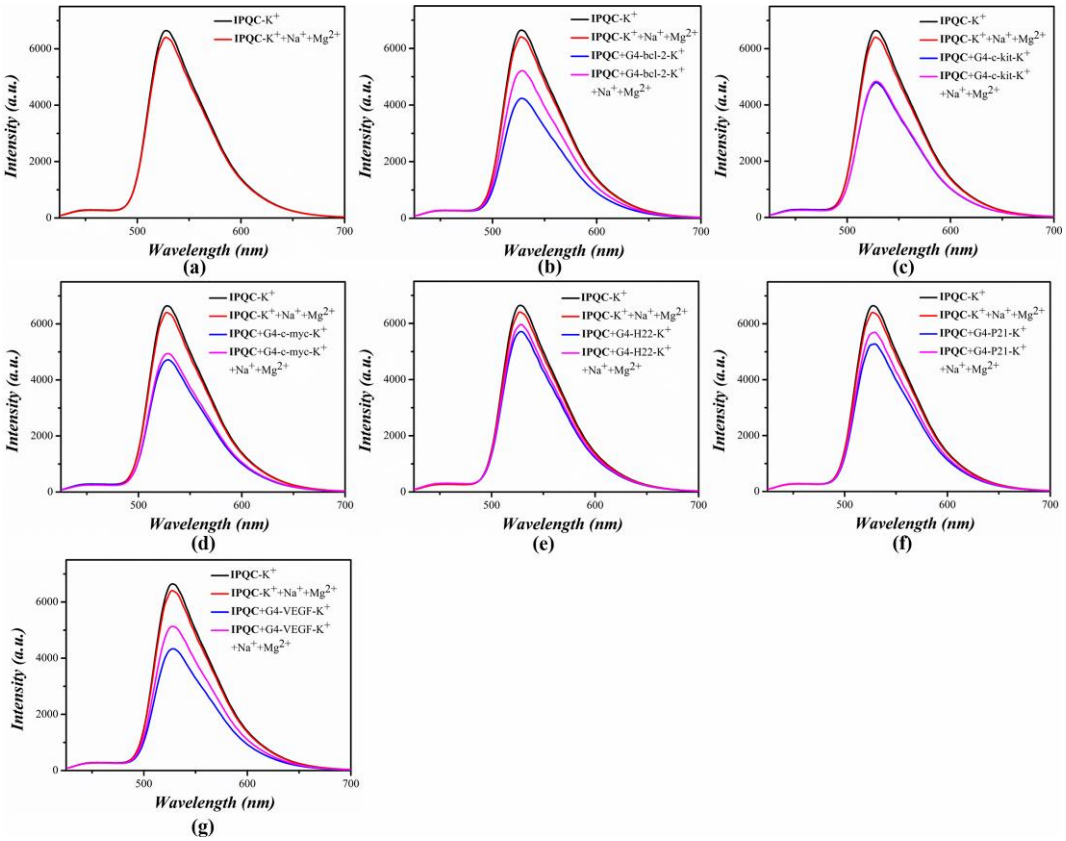

Figure S79 Fluorescence spectra of **IPQC** (2.00×10^{-5} M) with various G4 DNAs (2.00×10^{-5} M) adding in the presence or absence of 20 mM Mg^{2+} ($MgCl_2$) and 10 mM Na^+ (NaCl) in the mixture containing ethanol and Tris-HCl buffer ([KCl] = 150 mM; [Tris] = 20 mM; the ratio between ethanol and aqueous phase as 1:99, *v/v*, pH = 7.2).

Different cation atmosphere effect study in the interaction between **IPQC** and G4-VEGF

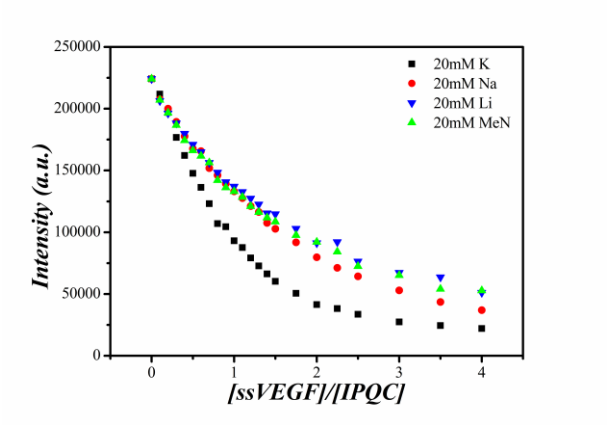

Figure S80 Fluorescence intensity change from 425 nm to 700 nm of the mixture containing **IPQC** (2.00×10^{-5} M) and increasing G4-VEGF in various salt solution. The black, red, blue and green plots show the change in 20 mM KCl, NaC, LiCl or Me_4NCl, respectively.

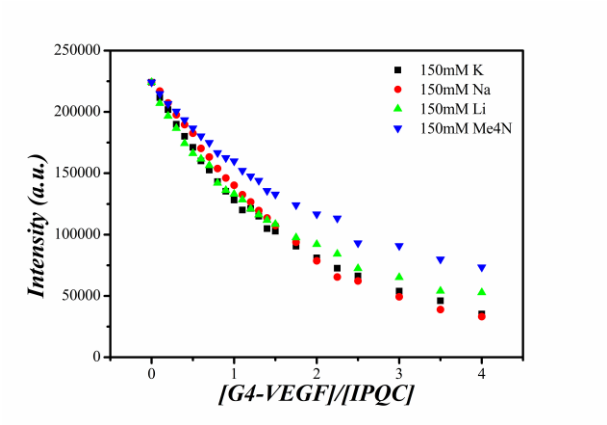

Figure S81 Fluorescence intensity change from 425 nm to 700 nm of the mixture containing **IPQC** (2.00×10^{-5} M) and increasing G4-VEGF in various salt solution. The black, red, blue and green plots show the change in 150 mM KCl, NaC, LiCl or Me_4NCl, respectively.

Study of K^+ concentration-dependent effect between **IPQC** and dsDNA.

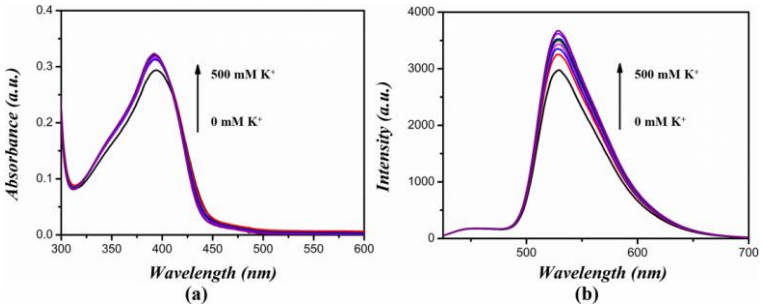

Figure S82 Changes in the Uv-vis absorption (a) and fluorescence emission spectra (b) of **IPQC** and ds20 as K^+ concentration varies from 0 to 500 mM in the mixture containing ethanol and Tris-HCl buffer ([Tris] = 20 mM; the ratio between ethanol and aqueous phase as 1:99, *v/v*, pH = 7.2).

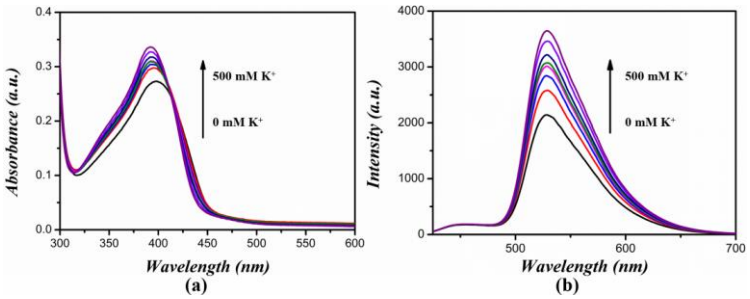

Figure S83 Changes in the Uv-vis absorption (a) and fluorescence emission spectra (b) of **IPQC** and ds22 as K^+ concentration varies from 0 to 500 mM in the mixture containing ethanol and Tris-HCl buffer ([Tris] = 20 mM; the ratio between ethanol and aqueous phase as 1:99, *v/v*, pH = 7.2).

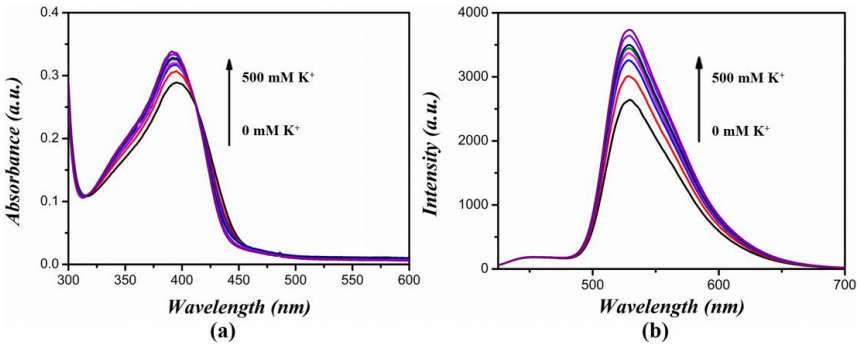

Figure S84 Changes in the Uv-vis absorption (a) and fluorescence emission spectra (b) of **IPQC** and ds26 as K^+ concentration varies from 0 to 500 mM in the mixture containing ethanol and Tris-HCl buffer ([Tris] = 20 mM; the ratio between ethanol and aqueous phase as 1:99, *v/v*, pH = 7.2).

Section S8: **References.**

(1) Sheldrick GM. SHELXT-Integrated space-group and crystal-structure determination. Acta Cryst. A., **2015**;71(1): 3-8.

(2) $Rw(F^2) = \{w(|F_O|^2 - |F_C|^2)^2/w(|F_O|)^4\}^{1/2}$ where w is the weight given each reflection. $R(F) = (|F_O| - |F_C|)/|F_O|\}$ for reflections with $F_O > 4((F_O))$. $S = [w(|F_O|^2 - |F_C|^2)^2/(n - p)]^{1/2}$, where n is the number of reflections and p is the number of refined parameters.

(3) Sheldrick GM. SHELXTL/PC (Version 5.03). Siemens Analytical X-ray Instruments. Inc., Wisconsin, USA, **1994**.

(4) Y.-F. Luo, T. Yang and Y.-Q. Wei, CN 107739375 A, 2018.

(5) N. Satish Kumar, L. Chandrasekhara Rao, N. Jagadeesh Babu and H. M. Meshram, *RSC Advances*, 2015, **5**, 95539-95544.

(6) M. Hagimori, S. Matsui, N. Mizuyama, K. Yokota, J. Nagaoka and Y. Tominaga, *Eur. J. Org. Chem.*, 2009, **2009**, 5847-5853.

(7) Job P. Formation and stability of inorganic complexes in solution. *Ann. Chim.* 1928, **9**, 113-203.

(8) Gans P, Sabatini A, Vacca A. Investigation of equilibria in solution. Determination of equilibrium constants with the HYPERQUAD suite of programs. *Talanta,* 1996, **43**, 1739-1753.

(9) Wei D, Parkinson GN, Reszka AP, Neidle S. Crystal structure of a c-kit promoter quadruplex reveals the structural role of metal ions and water molecules in maintaining loop conformation. *Nucleic Acids Res.,* 2012, **40**, 4691-4700.